NASA CONTRACTOR REPORT

NASA CR-1606

NASA CR-1606

A STUDY TO DEVELOP NEUTRON ACTIVATION FOR MEASURING BONE CALCIUM CONTENT

by H. R. Lukens, Jr., D. M. Fleishman, and J. K. Mac Kenzie

Prepared by
GULF GENERAL ATOMIC INCORPORATED
San Diego, Calif.
for Ames Research Center

NATIONAL AERONAUTICS AND SPACE ADMINISTRATION • WASHINGTON, D. C. • JUNE 1970

NASA CR-1606

A STUDY TO DEVELOP NEUTRON ACTIVATION FOR MEASURING BONE CALCIUM CONTENT

By H. R. Lukens, Jr., D. M. Fleishman,
and J. K. Mac Kenzie

Prepared under Contract No. NAS 2-5178 by
GULF GENERAL ATOMIC INCORPORATED
San Diego, Calif.

for Ames Research Center

NATIONAL AERONAUTICS AND SPACE ADMINISTRATION

For sale by the Clearinghouse for Federal Scientific and Technical Information
Springfield, Virginia 22151 – CFSTI price $3.00

CONTENTS

TABLES

TABLES (continued)

FIGURES

A STUDY TO DEVELOP NEUTRON ACTIVATION FOR MEASURING BONE CALCIUM CONTENT

by

H. R. Lukens, Jr., D. M. Fleishman, and J. K. Mac Kenzie

SUMMARY

A study of the feasibility of utilizing neutron activation analysis for the in vivo determination of bone calcium in the macaque monkey has been carried out. Theoretical calculations showed that the absolute determination of bone calcium by in vivo neutron activation analysis is highly dependent on the use of comparator standards that accurately represent the size, shape, and composition of the specimen. This requirement, which was experimentally proven, is primarily dictated by neutron behavior in the specimen. Other factors are straightforward, as has been demonstrated by a number of authors.

Accurate models of a vertebra and a femur were constructed of calcium-loaded plastic, and analyses of two vertebrae and a femur were carried out under simulated in vivo conditions (total radiation doses of 1.5 rem in most cases, and about 6 rem in some cases) using the models as comparator standards. The absolute calcium values were confirmed by both high-flux neutron activation analysis and atomic absorption analyses. The average values (and standard deviations) of the three methods, in grams of calcium, were as follows: first vertebra = 1.49 (±0.04), second vertebra = 1.59 (±0.08), femur = 8.30 (±0.11).

With sufficiently accurate comparator standards, it is estimated that in vivo neutron activation analysis is capable of determining absolute calcium levels in the whole body to within 2% to 3% of the actual value. Accuracies and precisions commensurate with the above experimental findings are expected in the analysis of selected portions of the body. Even better precisions are anticipated for observing relative changes of calcium in a given specimen by serial measurements. It is concluded that useful application of neutron activation analysis for in vivo calicum determination in the macaque monkey is feasible.

INTRODUCTION

The work described in this report consisted of a study of the feasibility of utilizing neutron activation analysis for the in vivo determination of bone calcium in the macaque monkey. The author wishes to acknowledge at the outset the cooperation of Dr. Donald R. Young of the Biomedical Research Branch of the National Aeronautics and Space Administration Ames Research Center, Technical Monitor of the contract under which this work was performed, who provided material and suggestions which contributed to the success of the program.

As stipulated by the terms of the contract, the work was divided into two phases. Phase A consisted of a theoretical treatment and a literature survey concerning the most suitable equipment and procedures for measuring the calcium in selected parts of the body and in the whole body of a macaque monkey, especially M. nemestrina, weighing about 10 kg. Phase B consisted of (1) experimental confirmation of the sensitivity and reproducibility of the neutron activation analysis method for determining calcium in known standards of varying calcium content, and (2) determination of the calcium in a femur and vertebra of the macaque monkey by neutron activation analysis, with analytical confirmation by an independent assay.

Although not specifically stipulated in the contract, the major portion of Phase B was carried out at radiation levels acceptable for in vivo application. Femoral and vertebral standards were prepared from molds of actual bone specimens to have exact exterior dimensions. Both the standards and the bones were irradiated with neutrons from a nuclear reactor in such a manner that they received total radiation doses, consisting of thermal neutrons, fast neutrons, and gamma rays, of less than 6 rem in any single experiment. Following neutron activation, each irradiated specimen was examined by gamma-ray spectrometry to obtain an estimate of the amount of radioactive calcium, specifically Ca^{49}, that had been formed during the irradiation by the $Ca^{48}(n,\gamma)Ca^{49}$ reaction.

The procedures used in Phase B were derived from the findings of Phase A plus unpublished data available at this laboratory. In addition to the development and application of a practical procedure for the analysis of actual bones on an in vivo basis, experiments were carried out to indicate the effects of tissues of various thicknesses and in various positions adjacent to bones.

For the reader who may not be acquainted with neutron activation analysis, a brief description of the method is given below. The remainder of the report consists of descriptions of Phases A and B of the program, followed by a discussion of the results obtained.

Neutron activation analysis utilizes neutron-induced nuclear reactions to form radionuclide species that can be used as analytical indicators. A useful indicator can be formed from at least one of the naturally occurring isotopes of most of the elements, and the decay characteristics of each indicator radionuclide species are peculiar enough to that species to allow unequivocal identification and quantitation. Other factors being equal, the amount of a particular indicator radionuclide species produced by the neutron irradiation of a certain element in a sample will be linearly proportional to the amount of that element in the sample.

An important characteristic of a radionuclide is its half-life. Starting with a given number of atoms of a radionuclide species, only half of that number will remain after a one half-life period of time. The atoms disappear, of course, by radioactive transformations, wherein they give up energy in the form of emitted radiations as they are transformed into a different nuclide species. The most convenient way of measuring the number of atoms of a radioactive species present in a given sample is to measure, with suitable instrumentation, the intensity of the characteristic radiation of the species emitted from the sample. The radiation intensity is often spoken of as "radioactivity" or "activity," and the activity, A, is related to the number, N^*, of radioactive atoms of a given species by the equation

$$A = N^* \frac{0.693}{t_{1/2}} \quad (1)$$

where $t_{1/2}$ is the half-life of the species.

Fundamental Equation of Neutron Activation Analysis

The activity of a radionuclide species that is formed from a precursor nuclide species in a sample by a neutron-induced reaction is given by the equation

$$A_o = N\phi\sigma \left(1 - e^{-0.693t_i/t_{1/2}}\right) \quad (2)$$

where A_o = the activity at the end of the irradiation,

t_i = the duration of the irradiation,

$t_{1/2}$ = the half-life of the radionuclide species,

N = the number of atoms of the precursor species in the irradiated sample,

ϕ = the flux of neutrons impinging on the sample during the irradiation,

σ = the so-called "cross section" of the reaction.

The parenthetical term in Eq. (2) is called the "saturation factor."

The reaction cross section, σ, is usually given in cm^2/nucleus. It defines the probability that the particular reaction will be produced by neutrons of a particular energy. Furthermore, the reaction cross-section value varies with neutron energy. Hence, where the neutron flux value, which is usually expressed as neutrons/cm^2/sec, is given for a particular

energy of neutrons, the cross section value appropriate to that energy of neutrons should be used. Where the flux value applies to neutrons having a range of energies, the appropriate "effective" cross-section value should be used.

Neutron Sources

The two most commonly used sources of neutrons for activation analysis are the research nuclear reactor and the Cockroft-Walton generator.

The reactor produces high fluxes of neutrons by the nuclear fission process, which gives rise to neutrons having an energy spectrum of from a small fraction of a million electron volts (MeV) to around 20 MeV. The average energy of the fission-spectrum neutron is about 1.5 MeV. For reasons of neutron economy, the majority of fission-spectrum neutrons are moderated (reduced in energy via elastic and inelastic collisions) to ambient temperature energies, after which they are spoken of as "thermal neutrons." Thermal neutrons have an average energy of about 0.025 eV (at about 20°C). The result is that fluxes of both fission-spectrum and thermal neutrons exist in the reactor core. For example, in the outermost ring of fuel elements in a Gulf General Atomic TRIGA Mark I reactor, there are fission-spectrum and thermal-neutron fluxes of 3.5×10^{12} n/cm^2-sec and 2.5×10^{12} n/cm^2-sec, respectively, when the reactor is operating at 250 kW.

The Cockroft-Walton generator in most prevalent use accelerates deuterium ions to 150 to 200 keV, after which they are impinged on a tritiated metal target. This affects the $H^3(H^2,n)He^4$ reaction, and the neutrons produced have energies close to 14 MeV. Machines costing $20 000 to $25 000 (roughly 10% of the cost of a reactor) can produce a total of 1×10^{11} to 2.5×10^{11} 14-MeV neutrons per second. The neutrons travel in all directions from their point of production, so the actual fluxes of 14-MeV neutrons attainable at a sample position are on the order of 10^9 n/cm^2-sec. Because thermalization requires a geometry sacrifice (for insertion of moderating

material) in proportion to the fraction of neutrons thermalized, only comparatively modest thermal-neutron fluxes, on the order of 10^7 n/cm^2-sec, can be obtained; and, except when the geometry sacrifice is very great, the high-energy neutron flux remains substantially high.

Other devices, such as Van de Graaff generators, cyclotrons, betatrons, and electron linear accelerators, can also be used to generate neutrons. However, these are less commonly used than the two sources discussed above, owing to such factors as their comparatively poor availability, high initial cost, or relatively poor neutron output.

Radioactivity Measurement

With only a few exceptions, useful analytical indicator radionuclides that emit gamma rays can be produced from elements by neutron activation. Gamma rays have the characteristic of being both monoenergetic and highly penetrating. The latter property is important in the measurement of radioisotopes in samples of reasonable size. The former property provides for qualitative identification, since the gamma rays from each species of emitter have unique energies. No other type of radiation from radionuclides has these properties. Although x-rays, which arise from some modes of decay, are monoenergetic, in general they have insufficient energy for suitable penetration.

Two kinds of detectors are in common use for the measurement of gamma rays: the thallium-activated sodium iodide crystal and the lithium-drifted germanium detector. The former converts and reemits a certain fraction of absorbed gamma-ray energy as visible and near-visible light, the amount of light emitted being directly proportional to the amount of absorbed gamma-ray energy. A multiplier phototube is used to convert the emitted light

into an electrical pulse that is still proportional in strength ("height," in more common parlance) to the gamma-ray energy deposited in the NaI(Tl) crystal.

A Ge(Li) detector operates as a reverse-bias transistor, and it momentarily produces an electrical pulse when ions are formed within its sensitive region by the action of gamma rays. The electrical pulse is proportional in height to the gamma-ray energy deposited in the sensitive region of the device.

Electrical pulses from either device may be linearly amplified and measured with a pulse-height analyzer. The modern multichannel pulse-height analyzer divides the pulse-height spectrum into narrow channels corresponding to a few keV of gamma-ray energy, sorts the incoming pulses of all energies into the channels corresponding to their energies, and stores them in corresponding locations in a magnetic-core memory. A means of accounting for the number of pulses stored in each memory channel is also provided.

A gamma ray may deposit all of its energy in a detector, in which case the resulting pulse will be stored in one of a limited number (the number depending on the resolution of the spectrometer system) of channels. However, an appreciable fraction of gamma-ray interactions are such that the gamma ray is scattered out of the detector after deposition of only part of its energy. Because of the variability of deposited energy that results from such events, the resulting pulses are distributed among a large number of channels. Hence, the gamma-ray pulse-height spectrum of a sample will display a continuum of responses corresponding to scattering events, above which will be seen peaks corresponding to complete deposition events.

NaI(Tl) detectors are available in larger sizes than Ge(Li) detectors. A commonly used 7.6-cm-diameter by 7.6-cm-long NaI(Tl) detector has a volume of about 345 cc, while the largest available Ge(Li) detectors have a volume of only about 50 cc. Thus, although the Ge(Li) detector systems have much better energy resolution than the NaI(Tl) detector systems, the latter are

much more efficient with respect to the absorption of total gamma-ray energy, especially in the case of the high-energy gamma rays that are of interest in the present program.

In a gamma-ray spectrum, the peaks have both qualitative and quantitative value, and the rate at which counts are recorded in a peak (the peak counting rate) is related to the rate at which the corresponding gamma rays are being emitted from the sample by an efficiency factor. The peaks, peak counting rates, and peak counting efficiencies are generally termed "photopeaks," "photopeak" counting rates, and "photopeak" counting efficiencies, respectively, since the photoelectric process is the dominant means of total gamma-ray absorption in the detector (or, for higher gamma-ray energies, Compton scattering followed by photoelectric absorption).

The photopeak counting efficiency is a function of the kind and size of detector employed, the gamma-ray energy, the geometric relationship between the sample and the detector, and the fraction of disintegrations that lead to emission of the gamma ray in question (the gamma-ray yield). The latter factor derives its importance from the fact that certain radionuclide species do not emit a particular gamma ray in every disintegration. For example, Ca^{49} emits a 3.10-MeV gamma ray in 89% of its disintegrations, rather than in every disintegration.

Where the photopeak counting efficiency factor is E, Eq. (2) may be expressed to give the photopeak counting rate, R:

$$R = EN\phi\sigma\left(1 - e^{-0.693t_i/t_{1/2}}\right) \qquad (3)$$

Analytical Practice

The photopeak counting rates that can be expected with a given gamma-ray spectrometer system, following an irradiation of specified flux and duration, can be calculated with Eq. (3). Conversely, where all system parameters are

defined, Eq. (3) may be used to determine N, where R has been measured. In this case, since some appreciable decay of the radionuclide being measured may occur from the end of the irradiation to the effective time of the counting period, it may be necessary to make a decay correction in accordance with the following equation:

$$R = R_o e^{-0.693 t_d / t_{1/2}} \qquad (4)$$

where R_o = the photopeak count rate at the end of the irradiation,

R = the photopeak count rate at the time of the counting period,

t_d = the time interval between the end of the irradiation and the counting period.

Once N has been determined, the amount of the element present in the sample is easily derived from the fact that each of the various stable isotopes of each element occurs in nature in a well-defined fraction of the total. For example, the isotope Ca^{48}, which is the precursor species of Ca^{49} in the $Ca^{48}(n,\gamma)Ca^{49}$ reaction, makes up 0.185% of naturally occurring calcium. Therefore, the number of Ca^{48} atoms determined to be in a sample may be divided by 0.00185 to obtain the total number of calcium atoms in the sample.

A more common practice is to use comparator standards containing known amounts of the elements to be determined. If the comparator has the same geometry and neutronic properties as the sample, and if it is irradiated and counted in exactly the same way as the sample, then the count rate of the appropriate photopeak of the sample may be compared with that of the standard to obtain a quantitative analysis. This procedure avoids the necessity of knowing the precise values of the flux, cross section, photopeak counting efficiency, etc., and better accuracy and precision are the result.

PHASE A

Preliminary Considerations

Calcium activation.— Computations have been made of the gamma-ray photopeak counting rates that are obtainable with a 7.6-cm-diameter by 7.6-cm-long NaI(Tl) detector, coupled to a multichannel pulse-height analyzer, subsequent to a 1-hr irradiation of 1 g of each of the stable elements in the TRIGA Mark I nuclear reactor (ref. 1). In these calculations, which covered 896 reactions, the thermal-neutron and fission-spectrum neutron fluxes in the irradiation position were each taken to be 3.5×10^{12} n/cm^2-sec. Thermal-neutron reaction cross sections were taken from Hughes and Schwartz (ref. 2), and fission-spectrum neutron reaction cross sections from Roy and Hawton (ref. 3). Photopeak counting efficiencies were computed from NaI(Tl) response efficiency data given by Heath (ref. 4) and the gamma-ray yields given by Strominger, Hollander, and Seaborg (ref. 5). The sample size was taken as 1 cc (approximately equidimensional); and the source-to-detector distance was that obtained when the detector was covered with a 1.25-cm-thick plastic beta-particle absorber, with the sample placed on top of the absorber.

The reactions that lead to the production of gamma-ray emitting radionuclides from the six stable calcium isotopes and the computed photopeak counting rates obtained from 1 g of calcium under the above conditions are given in table 1. Clearly, the $Ca^{48}(n,\gamma)Ca^{49}$ reaction provides the greatest sensitivity for the determination of calcium. Furthermore, the 3.1-MeV gamma ray emitted by Ca^{49} falls in a spectral region that is subject to little interference from gamma rays of radionuclides derived from reactor neutron irradiation of other elements present in biological tissue. Also, the 3.1-MeV gamma ray is more penetrating than the weaker gamma rays of the other product isotopes, which minimizes matrix effects in the examination of large samples.

The 14-MeV neutrons from a Cockroft-Walton generator are generally not used to determine calcium by activation analysis. Using the cross-section

values listed by Kenna and Conrad (ref. 6), one can compute that a 14-MeV neutron flux of 10^9 n/cm^2-sec will produce less than 10% of the amount of any radionuclide activity from calcium than can be obtained with a reactor, and the amount of Ca^{49} produced will be many orders of magnitude less. Thus, the best means of measuring calcium with such a generator is to utilize hydrogenous material to moderate the neutrons so that thermal neutrons will be available to most efficiently promote the $Ca^{48}(n,\gamma)Ca^{49}$ reaction. From Eq. (3), it can be seen that if a thermal-neutron flux of 3.5×10^{12} n/cm^2-sec can produce 1.4×10^8 photopeak cpm of Ca^{49} per gram of calcium (table 1), then a thermal-neutron flux of 10^7 n/cm^2-sec (which is usually the best that can be achieved with a small Cockroft-Walton machine) will produce only 4.0×10^2 photopeak cpm of Ca^{49} per gram of calcium.

However, the relatively poor Ca^{49} yield from a Cockroft-Walton generator, compared with that from a reactor, is not per se sufficient reason to rule out the use of such a generator in the present work, since radiation-dose considerations preclude the use of maximum reactor fluxes for in vivo investigations.

Radiation dose.— A listing of the probable effects of various acute radiation dosages over the whole body indicates that no effect can be expected from 0.3 R, no obvious injury or readily detectable effects are likely up to 25 R, and possible blood changes (but no readily detectable or serious injury) can be expected from doses of 25 to 50 R (ref. 7). The maximum permissible chronic, whole-body dose is defined as 1.25 rem per calendar quarter (ref. 8). This information is useful in determining the radiation levels that are acceptable when studying the bone calcium of the macaque monkey by in vivo neutron activation analysis, especially where serial measurements are to be made. The fact that blood changes are among the first noticeable effects of excessive radiation implies damage to biological mechanisms residing in the bone. Hence, it is suggested that acute doses given in bone-study work be kept well below 25 rem, and preferably not much above the maximum permissible adult human dose.

The relative biological effectiveness (RBE) of gamma rays is unity. Therefore, roentgen measurements of gamma-ray doses are equivalent to rem values. In contrast, the RBE of neutrons is greater than unity, and varies with their energy. In terms relevant to the applications of neutrons in the present study, the integrated neutron fluxes of neutrons of various energies required to deliver 1 rem are given in table 2, which is taken from the Federal Register (ref. 8). It can be seen from table 2 that dose considerations, in addition to analytical-indicator formation considerations, favor the use of thermal neutrons over the use of either 14-MeV neutrons or fission-spectrum neutrons.

From a practical standpoint, an irradiation should not be too brief to allow accurate timing. On the other hand, high saturation factors are obtained for the production of Ca^{49} rather quickly (75% saturation in 17.6 min; see Eq. (2)). Based on these two factors, the optimum range of thermal-neutron fluxes for the present work is on the order of 10^6 to 10^7 n/cm^2-sec. A thermal-neutron flux of 10^6 thermal n/cm^2-sec will deliver 1 rem in 16.1 min and produce 29 photopeak cpm of Ca^{49} per gram of calcium (when counted with a 7.6-cm by 7.6-cm NaI(Tl) detector); and a thermal-neutron flux of 10^7 n/cm^2-sec will deliver 1 rem in 1.61 min and produce 47 photopeak cpm of Ca^{49} per gram of calcium.

Examination of neutron behavior shows that a beam composed solely of thermal neutrons suffers appreciable flux attenuation in hydrogenous materials. This effect can be partially offset by the presence of more energetic neutrons that become thermalized within the sample. Hence, a beam containing neutrons with energies ranging from thermal to <10 keV is desirable.

Neutron behavior.— Since somewhat different considerations apply to thermal and fast neutrons, these categories are discussed separately below.

Thermal neutrons: Although the species H^1 has a rather low atomic cross section for the capture of thermal neutrons (3.3×10^{-25} cm^2/nucleus), its

concentration in biological tissues is sufficiently great to effect a significant amount of thermal-neutron capture.* Thermal-neutron flux attenuation by this process is described by the expression

$$I = I_o e^{-n\sigma x} \tag{5}$$

where I_o = the incident thermal-neutron flux,

x = the distance the neutron travels from the point of incidence,

I = the thermal-neutron flux at distance x from the point of incidence,

n = the number of absorbing atoms per cc of material,

σ = the atomic cross section for capture of thermal neutrons.

The concentration of hydrogen in wet tissue is nearly the same as that of water, namely 6.7×10^{22} atoms/cc. Therefore, from Eq. (5), as a result of neutron capture, an incident thermal-neutron flux will be reduced by 2.2% after traveling through 1 cm of tissue. The mean free path (i.e., the average total scalar distance a neutron will travel before it is absorbed) of thermal neutrons in water is 45 cm.

While flux attenuation by absorption is significant, loss of thermal neutrons from samples of limited size by scattering and leakage is more serious. The atomic cross section of hydrogen for the scattering of thermal neutrons is 3.5×10^{-23} cm^2 per atom. Thus, from Eq. (5), 50% of the neutrons

---

*The atomic cross sections of carbon and oxygen for thermal-neutron capture are 3.7×10^{-27} and $<2 \times 10^{-28}$ cm^2/nucleus, respectively. Therefore, these elements may be ignored in discussing flux attenuation by thermal-neutron capture. Other elements, which have much smaller concentrations in biological tissue, can also be ignored.

incident on wet biological tissue will be scattered within the first 0.3 cm of travel. This distance may be called the average path length.

Since the binding energy of hydrogen in most chemical bonds amounts to several electron volts, a thermal neutron (0.025 eV) does not have sufficient energy to cause much displacement of a hydrogen atom. Therefore, from classical considerations, the average scattering angle for neutron scattering in biological material may be taken to be 90°. The result is, on the average, that an array of squares, with 0.3-cm sides, may be used to analyze neutron-beam distribution approximately.

Consider, for example, a disc of tissue-equivalent material that is 0.5 cm thick and 2.22 cm in diameter, with a thermal-neutron beam normal to, and homogeneously falling on, the circular face of the disc. One half of the incident neutrons will fall within a radial distance of 0.78 cm from the center of the disc face, and one half of the incident neutrons will fall outside of that distance; i.e., the circle defined by the 0.78-cm radius defines the line of average incidence. Neutrons falling on this circle will have a 50% chance of being scattered in the first 0.3 cm of path; 25% will be scattered toward the center of the disc and 25% will be scattered toward its edge. Of those scattered sideways, 12.5% will be lost from the edge of the disc, and 19.75% will be scattered out of each face of the disc. Thus, of the incident neutrons, $\sim$68% will go through the disc, $\sim$18% will be scattered back out of the entrance face, and $\sim$13% will be lost out of the side of the disc.

Although the above distribution analysis is oversimplified, it illustrates how much more effective scattering is than absorption in attenuating a thermal-neutron flux in small specimens of hydrogenous material.

Fast neutrons: As with thermal neutrons, elastic-scattering interactions are much more important than the absorption process in the behavior of fast neutrons in hydrogenous material. A fast neutron loses energy in each scattering event; thus, scattering serves to moderate fast neutrons, in addition to effecting their dispersal.

The average value of the decrease in the natural logarithm of neutron energy per elastic-scattering event, which may be denoted by Δ, is 0.925 for water. That is, on the average, the energy of a fast neutron is reduced by a factor of 2.53 per scatter in water. If the difference between the natural logarithms of the average initial and final energy states of neutrons is divided by Δ, one obtains the average number of collisions required to effect the overall energy change in question. For example, thermalization of fission neutrons involves an energy change of from 1.5 MeV (average) to 0.025 eV; and

$$\frac{\ell n \left(\frac{1.5 \times 10^{6}}{2.5 \times 10^{-2}} \right)}{0.925} = 18 \text{ collisions to thermalize}$$

Similarly, an average of 20 collisions are required to thermalize 14-MeV neutrons.

The atomic scattering cross sections of hydrogen for 14-MeV neutrons and 1.5-MeV neutrons are 6.8×10^{-25} and 3.4×10^{-24} cm^2/nucleus, respectively. Corresponding cross sections of oxygen are about 1.5×10^{-24} cm^2 and 3×10^{-24} cm^2, but the energy loss to a neutron in a collision with oxygen is much less, on the average, than in a collision with hydrogen. Similar considerations apply to less abundant constitutents of tissue, such as carbon and nitrogen. Thus, in tissue, a 14-MeV neutron has a 50% chance of traveling about 15 cm before it suffers its first important energy loss; and a fission neutron will travel about 3 cm, on the average, prior to its first important collision.

Clearly, since generator-produced 14-MeV neutrons arise from a small area of target, severe geometric penalties are imposed when an attempt is made to obtain from such a source a neutron beam of the desired qualities, i.e., a beam with a high ratio of low-energy to high-energy neutrons. These penalties are much less severe in the case of a reactor and, because of the much higher neutron output of a reactor, can be more readily tolerated.

Because of the wide spread of fission-neutron energies, and because of the significant loss of energy in the first few collisions, the scattering

cross section of 1- to 10 000-eV neutrons (namely, 2.2×10^{-23} cm^2) can be used with good accuracy in describing the thermalization of fission neutrons. The total average scalar distance, D, traveled by neutrons during thermalization is expressed by the equation

$$D = \frac{\text{No. collisions to thermalize}}{(n)\ (\sigma)} \tag{6}$$

Thus, fission neutrons travel an average of 12.2 cm (scalar distance) during thermalization in water. The corresponding net vector distance to thermalization is slightly less than one-half the scalar distance. Since a typical reactor core has a diameter and length each >1.5 ft, it can be seen that an appreciable fraction of neutrons leaving the reactor are already thermalized.

Further neutron-spectrum shaping can be obtained by the use of moderating material external to the core of the reactor.

Potential interferences.— Few elements in the body have the proper combination of concentration, suitable activation cross section, and gamma-emitting activation products to offer serious potential interference in the determination of calcium. Examination of the elements which compose the body (ref. 9), in conjunction with the neutron-activation products of the various elements present (ref. 1), shows that no interference to be expected will render the neutron activation method inapplicable for the determination of calcium. The most significant activation products are given in table 3, with their characteristics and the specific activities from a 10-min irradiation of body tissue at a thermal-neutron flux of 3.5×10^6 n/cm^2-sec. It can be seen that the 3.1-MeV gamma ray of Ca^{49} exhibits a higher specific activity than the nearest potentially interfering intense gamma ray, the 2.75-MeV gamma ray of Na^{24}. Gamma-ray spectrometry can easily resolve these two gamma rays to give an almost interference-free analysis.

The activation product S^{37} has a gamma ray of nearly the same energy as that of Ca^{49}. However, the S^{37} arising from sulfur via the $S^{36}(n,\gamma)S^{37}$

thermal-neutron reaction will amount to only about 0.25% of the Ca^{49} yield from calcium. Another reaction, $Cl^{37}(n,p)S^{37}$, also gives rise to S^{37}. However, even with a fission-spectrum neutron flux equal to the thermal-neutron flux and with the same amounts of chlorine and calcium, the S^{37} yield is only 3.5% of the Ca^{49} yield. The amount of calcium in the body is ten-fold greater than the amount of chlorine, and the recommended neutron beam will have much fewer fission-spectrum neutrons than thermal neutrons. Therefore, the $Cl^{37}(n,p)S^{37}$ reaction is not expected to contribute more than a 0.1% error in the final result. In total, S^{37} will thus contribute something less than 0.35% of the total photopeak attributed to Ca^{49}.

Accuracy.— The level of calcium activity indicated in table 3 is reasonably encouraging. If a 10-kg monkey were exposed to a homogeneous thermal-neutron flux of 3.5×10^6 n/cm^2-sec for 10 min, and if the monkey could be counted with the same efficiency as a 1-cc sample with a 7.6-cm by 7.6-cm NaI(Tl) detector, then the 3.1-MeV photopeak count rate of Ca^{49} would be 12 000 cpm at the end of the irradiation. In a 10-min count, allowing for decay (Eq. (4)) while counting, 81 000 photopeak counts would be collected. The standard deviation of 81 000 counts, where the photopeak baseline is expected to contribute an additional $\sim$10 000 counts, would correspond to an uncertainty of only $\pm$0.56 g out of 150 g of calcium.

Of course, the size of the whole monkey actually precludes an optimum counting efficiency with a 7.6-cm by 7.6-cm counter. However, larger counters are available and may be used in a coupled array to achieve fairly good counting efficiencies. Even if only one-fourth of the counting rate cited above were realized, the standard deviation would be only $\pm$0.75% of the value.

A possible source of difficulty in achieving highly accurate results is the perturbation of the thermal-neutron flux caused by scattering in the specimen. This effect will probably preclude the uniform irradiation of all body parts. A detailed theoretical analysis of the variation in thermal-neutron flux at different points in the body of a macaque monkey would be quite difficult, and is beyond the scope of the present work. The leakage

of thermal and fast neutrons from the many diverse shapes such a specimen presents is not only complex, but it will differ with different specimen sizes and shapes. Also, an exact theoretical calculation would require an accurate knowledge of the neutron-energy spectrum in the neutron beam used to activate the sample. Therefore, in the present study several experiments were carried out in Phase B to provide data relevant to this subject.

Comparator standards.— The difficulty presented by nonuniform irradiation can be circumvented through the use of flux monitors, phantoms, or accurate comparator standards.

Flux monitors may be affixed to various points of the body to provide an indication of the true flux map. This method requires interpolation of the data to estimate the flux between monitoring points. Such interpolation poses problems, especially since it is not practical to mount monitors within the body.

Phantoms may be constructed with cylindrical bottles containing solutions of calcium. This method provides a measure of integrated flux over an artifact with the approximate exterior dimensions of the sample. Implicit in this method is the assumption that little effective error results from the contrast between sample heterogeneity and phantom homogeneity. This assumption is questionable in view of the previously discussed neutron scattering considerations and counting geometry considerations, which will be discussed later.

Accurate comparator standards may be constructed by using actual bones to make molds, and then using the molds to make models of the bones from a self-setting plastic into which a known amount of a calcium compound has been mixed. The bone models may then be covered with tissue-equivalent material in such a way that the dimensions and form of the represented body part are accurately duplicated. Such models will reproduce both the geometric and neutronic parameters of the samples that they represent. Hence, a minimum of assumptions and interpolations are associated with this type of comparator standard.

The accuracy with which comparator standards must be prepared deserves consideration with respect to measurement of induced Ca^{49}. The irradiation aspect of the technique is considerably less sensitive to minor inaccuracies, especially when a nuclear reactor is used, since the neutron beam is broad and homogeneous. However, a volume element of an activated, complex sample acts as an isotropic source with a geometric relationship to a radiation detector that may be quite different from that of many other volume elements.

Where the face of the detector presents a surface area, B to the radiation, and where the distance from a volume element of the sample to the detector face is x, the fraction, G, of radiation from the volume element that falls on the detector is given approximately by the expression

$$G = B/4\pi x^2 \tag{7}$$

The fraction G is often called the "geometry factor." The counting rate, R, obtained from a point source having a disintegration rate A will be

$$R = GA \tag{8}$$

(for 100% emission of gamma rays and a 100% detection efficiency).

Since the volume increments of the femur are distributed over a much greater space than those of the vertebra, it was decided to analyze the precision requirements of the femur model in terms of radial and longitudinal conformation. To a first approximation, the conformation of a thin cross section of the femur shaft may be likened to a ring. If the femur is counted with its long axis perpendicular to the radial axis of a cylindrical detector, the ring will be seen edge-on by the detector, as in figure 1.

Assuming that the total activity of the ring is equally distributed, the specific activity, S, in activity per radian, is given by

$$S = A/\Theta \tag{9}$$

where Θ is given in radians. The activity at any infinitesimal portion, P, of the ring will be (again, for 100% emission of gamma rays and 100% counting efficiency)

$$dA = Sd\Theta \tag{10}$$

and the counting rate observed from the increment will be

$$dR = GdA$$

or

$$dR \approx \frac{BSd\Theta}{4\pi r_2^2} \tag{11}$$

where r_2 is the distance from P to F.

With reference to figure 1, r_1 is the ring radius; x is the distance from the center of the ring to F; y intersects x at right angles, and divides x into segments x_1 and x_2; and Θ is the angle formed by r_1 and x. The following equalities provide a basis for the proper expression of r_2 in Eq. (11):

$$x = x_1 + x_2 \tag{12}$$

$$x_1 = r_1 \cos\Theta \tag{13}$$

$$x_2 = x - r_1 \cos\Theta \tag{14}$$

$$y = r_1 \sin\Theta \tag{15}$$

$$r_2 = (x_2^2 + y^2)^{1/2} \tag{16}$$

Substituting with Eq. (14) and Eq. (15) in Eq. (16) yields

$$r_2 = [(x - r_1 \cos\Theta)^2 + (r_1 \sin\Theta)^2]^{1/2}$$

$$= (x^2 - 2xr_1 \cos\Theta + r_1^2 \cos^2\Theta + r_1^2 \sin^2\Theta)^{1/2}$$

which simplifies to

$$r_2 = (x^2 - 2xr_1 \cos\Theta + r_1^2)^{1/2} \tag{17}$$

When Eq. (17) is used to substitute in Eq. (11), the result is

$$dR \approx \frac{BSd\Theta}{4\pi(x^2 - 2xr_1 \cos\Theta + r_1^2)} \tag{18}$$

With the assumption that $x^2 + r_1^2 = a$, and $-2xr_1 = b$, Eq. (18) takes the form for integration:

$$\int dR \approx 2 \cdot \frac{BS}{4\pi} \int_o^{\pi} \frac{d\Theta}{(a + b \cos\Theta)} \tag{19}$$

Thus,

$$R \approx \frac{1}{2} \frac{BS}{(a^2 - b^2)^{1/2}} \tag{20}$$

and

$$R \approx \frac{BS}{2(x^2 - r_1^2)} \tag{21}$$

Computation of count rates for ring sources using Eq. (21) shows that ring sources have nearly the same counting efficiency as point sources under reasonable counting conditions. For example, when a point source has an activity of 6.2832 gamma-ray dps (disintegrations per second) and is located 5 cm from the 45-cm^2 face of a detector, the counting rate computed from Eqs. (7) and (8) will be 0.90 cps (counts per second). If the same activity is distributed in a ring having a radius of 0.6 cm and its center located 5 cm from the same detector (r_1 = 0.6 cm and x = 5 cm, and S = 1 dps per radian

in Eq. (21)), the counting rate will be 0.91 cps.

From the foregoing, it can be inferred that a solid femur model will have very nearly the same counting efficiency as an identically placed actual femur. This is verified by a detailed examination of the counting efficiency of a cross-sectional portion of such a model, which appears as a solid disc.

The activity in a disc sample is distributed throughout the area, πr_1^2. The specific activity may be related to the radius of the disc with the differential of the expression Area = πr_1^2; i.e.,

$$\frac{d(\text{Area})}{dr_1} = 2\pi r_1 \tag{22}$$

Then the specific activity, S_d, can be expressed as

$$S_d = \frac{\text{Activity}}{2\pi r_1} \tag{23}$$

The count rate from the disc can be computed by substituting S_d for S and integrating Eq. (21) between $r_1 = 0$ and $r_1 = r_1$:

$$R = \int_o^{r_1} \frac{BS_d dr_1}{2(x^2 - r_1^2)} = \frac{BS_d}{4x} \ln\left(\frac{x + r_1}{x - r_1}\right) \tag{24}$$

For the case where B = 45 cm^2, x = 5 cm, and the activity is 6.2832 dps, values have been computed for count rates obtained for rings (Eq. (21)) and discs (Eq. (24)) of several radii. The results are as follows:

	Counting Rate, cps	
r_1, cm	Ring	Disc
0.2	0.902	0.900
0.4	0.904	0.901
0.6	0.910	0.903
0.8	0.924	0.908
1.0	0.936	0.912

It can be seen that a solid femur model (disc cross section) of the radius involved in the present study (0.6 cm) can be expected to provide a fairly accurate representation of the actual femur, which has a cross section intermediate between a disc and a true ring.

Based on the foregoing discussion, the long axis of an activated femur may be viewed as a line source of radioactivity. In order to achieve the best geometry, such a source is usually placed with its long axis parallel to the face of the radiation detector, as shown in figure 2. The specific activity, S, of such a source is obtained by dividing the total activity by the length of the source; i.e., $S = A/2Y$ in figure 2.

The counting rate, R, of such a source is given by

$$R = \frac{BS}{4\pi} \int_{-Y}^{Y} \frac{dy}{x^2 + y^2}$$

$$= \frac{BS}{2\pi} \int_{o}^{Y} \frac{dy}{x^2 + y^2} \qquad (25)$$

where B is the face area of the detector, x is the distance from O (the center of the line source) to the center of the detector face, and y is the distance from the center of the line to the line segment dy.

The integral of Eq. (25) is

$$R = \frac{BS}{2\pi x} \tan^{-1} \frac{Y}{x} \tag{26}$$

Thus, for a 20-cm line source (the length of the femurs used in this work) located 5 cm from a 45-cm^2 detector and a total gamma-ray activity of 2π dps, the count rate will be

$$R = \frac{2\pi}{20} \cdot \frac{45}{2\pi} \cdot \frac{1}{5} \cdot \tan^{-1}\left(\frac{10}{5}\right)$$

$$= (0.45)(1.11)$$

$$= 0.50 \text{ cps}$$

Clearly, the femur model must have very nearly the same length as the true femur.

From the foregoing it can be seen that although faithful reproduction of exterior dimensions, including any protuburances, is required in the construction of models of bones, very minor errors derive from the use of a homogeneous matrix.

Literature Survey

The indicator radionuclide used in the measurement of calcium in bone is not always Ca^{49}. For example, Soremark and Bergman used Ca^{47} generated in a 20-hr irradiation at a thermal-neutron flux of over 10^{12} n/cm^2-sec for the simultaneous and destructive measurement of calcium plus numerous other elements in mandibular bone (ref. 10). Nevertheless, because of considerations already discussed, Ca^{49} is the indicator chosen for the present in vivo applications. This choice is substantiated by published reports on the subject.

The use of neutron activation analysis for the in vivo determination of selected elements in body tissues has been examined by several investigators. In 1963, Maletskos, Osborn, and Braun (ref. 11) reported using a thermal-neutron beam (the thermal-neutron to fast-neutron flux ratio was about 1000) to activate a model "finger" consisting of a Lucite cylinder containing ~23% W calcium, which was surrounded by a cylinder of simulated flesh "Lucite," to study the feasibility of using the technique to measure bone calcium. They reported that the calcium value was 15% greater than values predicted from flux measurements, but expected that a detailed theoretical analysis would reduce the error to within 5%. The analytical indicator used was Ca^{49}.

In 1964, Anderson et al. (ref. 12) reported using 14-MeV neutrons from a Cockroft-Walton generator to measure sodium, chlorine, and calcium in humans. In the system described, the 14-MeV neutrons were moderated by the hydrogenous material of the subject and adjacent polyethylene slabs that were 3 cm thick. The resulting thermalized neutrons produced Na^{24}, Cl^{38}, and Ca^{49} by neutron-capture reactions with the corresponding elements, and these radionuclides were measured by gamma-ray spectrometry. A phantom consisting of 10 cylindrical polyethylene vessels, containing a total of 59 liters of solution, was used for calibration purposes. The solution contained sodium and chloride salts, but no calcium salt. The sodium, chlorine, and calcium values reported for two healthy humans of about the same age were as follows: total-body sodium, 82±3 g and 77±3 g; total-body chlorine, 90±7 g and 70±9 g; total-body calcium, 1500±300 g and 1140±140 g. Although these values, especially the calcium values, may be questioned on the basis of their disparity and the fact that no independent means of measurement was possible, the authors indicated that the method for determining calcium could be developed so as to have considerable value in studies of bone disorders and drug action.

In 1965, Lenihan pointed out that a thermal-neutron dose of 10^{10} n/cm^2 delivered to the thyroid would generate enough I^{128} (via the $I^{127}(n,\gamma)I^{128}$ reaction) to be measured by gamma-ray spectrometry, and would thus allow the in-vivo determination of iodine in the thyroid (ref. 13). Later, Lenihan et al. provided a preliminary demonstration of the validity of this approach,

albeit with rather high total radiation doses, by determining thyroid iodine in live sheep (ref. 14). They used I^{129} as an internal monitor, which was measured prior to activation and gave rise to measurable amounts of I^{130m} during the irradiation. About 90 rad of gamma-ray dose, 110 rad of thermal-neutron dose, and 1 rad of fast-neutron dose were delivered to each of two sheep. The I^{128} gamma rays were clearly discernible in postirradiation gamma-ray spectra. The in vivo analytical results were confirmed by subsequent analysis of extirpated thyroid tissue.

In 1967, Battye et al. described experiments relating to the use of 14-MeV neutrons for in vivo activation analysis (ref. 15). They pointed out that the method of Anderson et al. (ref. 12) contained a number of systematic errors relating to nonuniformity of irradiation, nonuniformity of counting geometry, and interfering reactions. They expressed doubts that a satisfactory solution of these difficulties was possible. In a discussion subsequent to this paper, it was pointed out that simultaneous biaxial rotation of the subject and a standard would be required to avoid the difficulties of nonuniform irradiation, including those arising from variations of 14-MeV neutron production from a Cockroft-Walton generator.

Also in 1967, Boddy and Alexander described their experimental attempts to measure thyroid iodine via activation analysis with 14-MeV neutrons (ref. 16). Their gamma-ray spectra had a very poor signal-to-noise ratio. That same year, Palmer et al. described a promising approach to the in vivo measurement of calcium (refs. 17 and 18). They used a cyclotron-produced low-level flux of fast neutrons to irradiate cadavers and phantoms, and passed the irradiated samples through a circular array of six 4-in.-diameter by 9-3/8-in.-long NaI(Tl) detectors. Their irradiation and counting times were 15 min and 12.5 min, respectively, and the authors estimated that the method could quantitate whole-body calcium with a standard error of ±5%.

The work described by Palmer et al. is the best indication found in the literature that in vivo neutron activation analysis is suitable for the determination of body calcium. Their work is notable for several reasons:

(1) an aqueous phantom containing a skeleton was used, so the phantom gave a better correspondence with an actual specimen than the usual homogeneous phantom; (2) the specimens and phantoms were formed in a circular arc to achieve more uniform incident radiation from the accelerator source of neutrons; and (3) a reliable method for absolute calibration was used. Despite these and other excellent features in the method of Palmer et al., there are some difficulties associated with the method: (1) the RBE of fast neutrons (>1 MeV) was taken as 5 by the authors, which is the RBE of thermal neutrons, and (as is apparent from Table 2) the RBE of fast neutrons is appreciably higher; (2) the primary fast-neutron beam produces sufficient amounts of S^{37} from chlorine to require a significant correction; and (3) the described thermal-neutron flux-gradient curves obtained by activating small vials containing manganese in a cadaver or phantom do not indicate the status of lateral gradients.*

Recently, Comar et al. described measurements of neutron-capture gamma rays to obtain in vivo determinations of the calcium-to-chlorine mass ratio of a human tibia (ref. 19). They utilized a curved 2-cm by 5-cm channel, formed of nickel-coated glass bricks, to obtain a pure beam of thermal neutrons from the Saclay reactor EL3. The neutron flux from this beam tube averaged 2×10^7 n/cm^2-sec and was entirely free of fast neutrons and gamma rays. In vivo irradiations of normal adult subjects were directed to the antero-internal face of the tibia. The dose rate was 0.23 rem/min, and irradiations of 10 to 30 min were performed. A 20-cc lithium-drifted germanium detector, coupled to a 4096-channel pulse-height analyzer, was used to measure capture gamma rays. These investigators did not report the accuracy or precision of their measurement, but they claim the calcium-to-chlorine ratio obtained was the same as that previously obtained by in vivo activation analysis with postirradiation counting (ref. 20).

The work of Comar et al. is interesting in that they have addressed

*Private communication indicates that these authors have examined lateral gradients and found them to be acceptable.

their attention to the measurement of elemental ratios. They reaffirm the essential impossibility of obtaining a uniform thermal-neutron flux throughout a large mass of tissue, and state that comparison of the radioactivity of an irradiated sample with that of an irradiated standard would be possible only if the standard faithfully reproduced the geometry and bulk composition of the sample--conditions they maintain are impossible to fulfill.

The attenuation of a thermal-neutron flux in tissue has been investigated with the use of phantoms by Fairchild (ref. 21). His work indicated that 2 cm of tissue attenuates the flux by a factor of 2.15. In a previously discussed paper (ref. 19), Comar et al. mention that their studies with phantoms indicate that the thermal-neutron flux is attenuated by a factor of 2 for each centimeter of tissue. The work described in the present report demonstrates conclusively that no simple attenuation factor is applicable in practice; rather, the attenuation factor is related to the geometry and dimensions of the sample.

A brief synopsis of papers presented this year in Glascow at an informal conference on the progress and problems of in vivo activation analysis was recently published (ref. 22). Unfortunately, insufficient details were included in the synopsis to allow a critique of the work described. It is hoped that these papers will be published in their entirety in the near future.

PHASE B

Equipment

Neutron sources.— The Gulf General Atomic TRIGA Mark I nuclear reactor was utilized as the chief neutron source for the present study. The reactor core is at the bottom of a 20-ft-deep pool of water and is surrounded by a graphite reflector. A 4-in.-ID pipe, with its lower end closed, was placed in a vertical position on top of the graphite reflector. The upper end of

the pipe protruded above the level of the water that is used for cooling, neutron moderation, and bulk shielding. Thus, the pipe formed a dry, vertical passageway for neutrons; i.e., it acted as a neutron-beam port.

When the reactor was operated at its rated steady-state power level of 250 kW, the thermal-neutron flux at the beam port was approximately 2×10^6 n/cm^2-sec. Measurements with gold foils indicated that the neutron-beam cadmium ratio for gold was six to one.

In addition, one of the 150-kV Cockroft-Walton accelerators at this laboratory was used to generate 14-MeV neutrons in order to obtain experimental data relating to the applicability of this type of neutron source in the present work.

Counting equipment.— Solid NaI(Tl) detectors were used in the measurement of the 3.1-MeV gamma ray that is emitted by Ca^{49}. A 12.7-cm-diameter by 12.7-cm-long detector was used whenever the greatest counting efficiency was desired. Otherwise, a 7.6-cm-diameter by 7.6-cm-long detector was used. A 7.6-cm-diameter by 7.6-cm-long detector with a well was used to measure Cu^{64} in activated copper foils. In each case, the detector was coupled to a 400-channel pulse-height analyzer, which permitted gamma-ray spectra to be obtained. Thus, it was possible to quantitate the desired radionuclide activity in the presence of other radionuclides that gave rise to gamma rays of other energies.

The 12.7-cm by 12.7-cm detector was located in an underground, cement-walled counting room, while the 7.6-cm by 7.6-cm detector was located in an aboveground counting room.

Animal bones.— The NASA Ames Research Center supplied two macaque monkey femurs and two macaque monkey vertebrae for this study. The femurs were about 20 cm long and had a shaft measuring about 7/8 in. in diameter at the mid-point of the length.

The initial weights of the single femur and the two vertebrae used in the bulk of the experiments were 37.7327 g and 8.1691 and 7.5271 g. However, it was observed that these weights changed with time, probably due to changes in moisture content.

Models.— Models of a femur and of a vertebra were constructed by mixing calcium carbonate in a self-setting resin and pouring the homogeneous mixture into rubber molds of the bones. Rubber molds were used to provide sufficient flexibility for nondestructive removal of the intact models after the mixture had hardened. The finished models were removed from the molds, allowed to dry at room temperature for 24 hr, and then oven-dried at 110°C overnight.

Five femur models with five different calcium contents and five vertebra models made with corresponding calcium contents were prepared. The characteristics of these models are given in table 4.

Additional samples.— Additional samples were prepared for experiments designed to provide supplementary information. One group of samples consisted of calcium-carbonate-loaded plastic cylinders, 1.4 cm in diameter by 4.6 cm long. These cylinders were covered with various amounts of hydrogenous materials for the purpose of investigating the effects of such materials on the neutron flux at the sample. One cylinder was left bare, and the rest were each encased in a 0.1-cm-thick polyethylene vial. Of the latter, one was used without the addition of further material; one was evenly covered with 0.15 cm of paraffin; two were covered semicylindrically with 0.15 cm of paraffin (including the ends); and three were evenly covered with 0.65 cm of paraffin, one completely and two semicylindrically (including the ends).

Seven discs, 2.22 cm in diameter by 0.5 cm thick, were prepared from polyethylene. The discs were then stacked, with copper foils, 1 cm by 1 cm by 0.008 cm thick ($\sim$75 mg) inserted between each pair of discs and at the top and bottom of the stack. The foils were centered on the long axis of the cylindrical stack.

Six discs, 7.6 cm in diameter by 0.5 cm thick, were prepared from nylon. These discs were stacked with 1 cm by 1 cm by 0.008 cm (∿75 mg) copper foils between each pair and at the top and bottom of the stack.

A 1-cc solution containing 5 μg of sodium and 50 μg of calcium, each as the nitrate, was prepared and sealed in a 2-dram polyethylene vial. This sample contained sodium and calcium in approximately the concentration ratio that is found in the primate body.

Two polyethylene vials, with a 1.8-cm ID and a 5-cm inside height, were substantially filled with $CaCO_3$ and then heat-sealed. These samples were used to examine the suitability of neutron activation with the Cockroft-Walton generator.

Sample holders.— Two types of sample holders were used: one type for holding samples in a fixed position, and another type for swinging samples back and forth. The latter type, two of which were built, was used for irradiation and counting of femur bones and models. All other samples were irradiated and counted in fixed position, except in one experiment that involved simultaneous irradiation of a femur and vertebra.

The fixed-position sample holders consisted of simple ring stands and clamps, with positioning marks, that allowed samples to be reproducibly positioned for irradiation and counting.

The swinging sample holder utilized a wheel, driven by an electric motor, with an offcenter pin to act as a cam shaft to drive a rod back and forth. Two versions were constructed. In one version, the cam wheel had a diameter of 7.6 cm and drove a short (6-in.) rod to which a 12-in. rod was connected with a universal joint. The longer rod was guided by a bearing to maintain a straight back-and-forth travel. This device passed an attached sample back and forth along a 7.6-cm line. Throughout the remainder of this report, this type of holder will be referred to as the "piston holder."

The second version of the moving holder utilized a 4.75-cm-diameter cam wheel to which a 25-cm rod was attached. This rod was attached at 12.5 cm from the fixed end of a 91-cm-long rod. The fixed end of the rod pivoted at a bearing, so that each revolution of the wheel caused the loose end of the 91-cm rod to be carried back and forth across a 37-cm-wide arc. This type of holder will be referred to as the "pendulum holder."

Since the speed at which the sample is swept across a fixed point is a sinusoidal function of the position of the cam, the sweeps effected by these holders are termed "sinusoidal sweeps."

Experiments

In all irradiations with the TRIGA Mark I nuclear reactor, the reactor was operated at 250 kW. All counts were timed by elapsed time as well as instrument live time; the former is used in decay corrections, and the latter gives the actual counting time by compensating for instrument dead time.

Femurs.— Irradiations of femur bone and models were carried out as follows. The bone was attached, with a clamp at its center, near the end of the 91-cm swinging arm of the pendulum holder. The position was adjusted so that at each end of a minimum horizontal swing across the 4-in. beam port, the entire 8-in.-long sample was out of the beam. The sample was always positioned so that the neck was horizontal and the condyles faced upward.

The holder arm was swumg so that the sample was not over the beam port at the start of the irradiation. The reactor was then brought to power, and the motor was turned on to swing the sample back and forth across the neutron beam. The time at the beginning of the irradiation and the duration of irradiation were recorded. Termination of the irradiation was effected by rapidly shutting down the reactor.

At the end of the irradiation, the sample radioactivity was monitored, and the sample was then removed to the counting station. At no time was a significant amount of radioactivity, from the health-physics viewpoint, encountered in these experiments.

At the counting station, the sample was attached to the arm of the piston holder, so that the sample was carried back and forth in front of, and at a constant and close distance from, the 12.7-cm by 12.7-cm NaI(Tl) detector. In one experimental series only, a pendulum holder was used to swing the samples back and forth across the face of a 7.6-cm by 7.6-cm NaI(Tl) detector. In all cases, the sample was positioned so that the side facing the detector was the same as the one that faced the neutron beam during the irradiation. The time at the beginning of a sample count, the "live" time of the count, and the "clock" time of the count were recorded. The accumulated gamma-ray spectrum was printed out on paper tape in digital form.

The oscillatory movement of the femurs during irradiation and counting, which was necessary because the samples were long relative to the diameters of the beam port and detectors, was not required in the irradiation of the other, shorter samples (such as the vertebrae and calcium-loaded cylinders).

After the femur had been analyzed by simulated in vivo measurements, it was sectioned into eight parts approximately as follows: (1) greater trochanter; (2) head; (3) neck and lesser trochanter; (4, 5, and 6) three sections of shaft; (7) medial condyle; and (8) lateral condyle. Each portion was placed in a separate 2-dram polyethylene vial, weighed, and analyzed by a standard instrumental neutron activation analysis procedure.

The analysis procedure was as follows. The portions and a comparator standard (known amount of calcium carbonate in a 2-dram polyethylene vial) were sequentially irradiated for 1 min in a thermal-neutron flux of 2.8×10^{12} n/cm^2-sec. After each irradiation, the sample was counted with a solid 7.6-cm by 7.6-cm NaI(Tl) detector coupled to a multichannel pulse-height analyzer.

Vertebrae.— In one series of experiments only, the pendulum holder was used to irradiate vertebra bone and models. In all other vertebra experiments, samples were reproducibly positioned on an aluminum plate over the neutron-beam port. In all cases, the processes of the sample faced to the side, and the beam was directed toward the ventral face of the body of the sample. A 1-cm^2 by 0.008-cm-thick copper foil was attached to the ventral face of the sample body to act as a flux monitor in some experiments.

Irradiation timing was the same as with the femur bone and models in the series where the samples were carried back and forth across the beam port. Where fixed positions were used, the sample was put in place, and the reactor was brought to power in as nearly a reproducible fashion as possible. However, it was necessary to use flux monitors to correct for differences in this step. When the reactor was at power, the time was marked, and then after an accurately timed period, the reactor was shut off.

The sample was then monitored, taken to a counting station, placed onto an NaI(Tl) detector, and counted. All important time parameters were marked and recorded, and the gamma-ray spectrum was recorded on paper tape in digital form. Copper flux monitors, when used, were counted in the NaI(Tl) well counter at 2 hr or longer after irradiation.

After the vertebrae had been analyzed by simulated in vivo measurements, they were sectioned into three parts (in a tray so that none of the material was lost): (1) central processes, (2) lateral processes and posterior (hard) part of the centram, and (3) balance of the centrum. Each portion was placed in a separate 2-dram polyethylene vial, weighed, and analyzed by a standard instrumental neutron activation analysis procedure.

The analysis procedure was as follows. The portions and a comparator standard (known amount of calcium carbonate in a 2-dram polyethylene vial) were sequentially irradiated for 1 min in a thermal-neutron flux of 2.8×10^{12} n/cm^2-sec. After each irradiation, the sample was counted with a solid 7.6-cm by 7.6-cm NaI(Tl) detector coupled to a multichannel pulse-height analyzer.

After the neutron activation analysis, the three portions of one vertebra were oven-dried and dissolved in hydrochloric acid. Each solution was made to a known volume in a volumetric flask with water and then analyzed by atomic absorption analysis. The second vertebra and the femur were similarly analyzed.

Other experiments.— The calcium-carbonate-loaded cylinders, with various amounts of adjacent hydrogenous material, were irradiated in fixed positions with the long axis of the cylinders perpendicular to the neutron beam. The cylinders were then counted with a 7.6-cm by 7.6-cm NaI(Tl) detector in the same fashion as the vertebrae, the part of the sample that faced the beam being placed adjacent to the detector. All important time parameters were recorded, and the gamma-ray spectra were recorded on paper tape in digital form. Copper foils in polyethylene vials were used to measure the integrated neutron flux in each experiment. Two hours or longer after the irradiation, the foils were counted with the NaI(Tl) well detector.

The stacked assembly of polyethylene discs was covered with 0.010 in. of cadmium, except for the bottom of the stack, which faced the neutron beam. The assembly was kept in a fixed position during a series of five vertebra irradiations. The vertebrae (bone and models, one at a time) and the stack were at separate positions over the beam, and the cadmium suppressed mutual contributions of scattered neutrons. Foils at the bottom of the vertebrae measured the incident neutron flux. The stack was dismantled after the irradiation, and the copper foils were counted with the NaI(Tl) well counter 2 hr or longer after the irradiation.

The stacked assembly of nylon discs was covered with 0.010 in. of cadmium, except for the bottom of the stack, which faced the neutron beam. In one experiment, the assembly was kept in fixed position over each of the five vertebrae (bone and models) that were irradiated sequentially in the same series of experiments in which the polyethylene discs were irradiated. The bottom of the stack was 1 cm above the body of the vertebrae. The stack was dismantled following the irradiation, and the copper foils were counted

with the NaI(Tl) well counter 2 hr or longer after the irradiation. In another experiment, the nylon discs were similarly irradiated with the following exceptions: (1) no vertebrae intervened between the beam and the discs; (2) in addition to the foils centered on the axis of the cylindrical stack, copper foils were placed on the bottom of the five lower discs at 2.8 cm from the axis; and (3) the irradiation was of 15-min duration (uninterrupted).

The 1-cc solution containing 5 μg of sodium and 50 μg of calcium was irradiated for 10 min in the rotary specimen rack of the TRIGA Mark I nuclear reactor. The thermal-neutron flux was 1.8×10^{12} n/cm^2-sec. Starting 4 min after the end of the irradiation, the sample was counted for 10 min with a 7.6-cm by 7.6-cm NaI(Tl) detector coupled to a multichannel pulse-height analyzer.

The Cockroft-Walton generator was used to generate 14-MeV neutrons in close proximity to $CaCO_3$ samples. Two configurations were used, in each of which the $CaCO_3$ was placed at the center of a cube of paraffin that was 10 in. on each side. The cube had two 3-in.-diameter access holes: one for placement of the sample, and the other for acceptance of the generator beam tube. In one configuration, the generator beam tube was brought to a distance of 1/8 in. from the sample, and the space between the tube terminus and sample was occupied by paraffin. In the other configuration, the beam-tube terminus was placed against the center of an uninterrupted side of the cube, so that the 3-1/4-in. distance between sample and terminus was occupied by paraffin. For each configuration, the irradiation was of 10-min duration, and a nearby BF_3 neutron-counter system was used to obtain relative integrated neutron fluxes.

The initial comparator standards used in the neutron activation analysis estimation of calcium in the sectioned bones were (1) calcium carbonate slurried in 5 ml of H_2O, and (2) 5 ml of dry calcium carbonate. These standards were later studied by neutron activation analysis to ascertain their reliability. This work was carried out with 1-min irradiations in a thermal-neutron flux of 2.8×10^{12} n/cm^2-sec, followed by gamma-ray spectrom-

etry. The dry $CaCO_3$ standards were run in duplicate, and they were compared with a different compound, calcium citrate. The slurried $CaCO_3$ standards, which were used only in the case of one vertebra, were run in triplicate to check the reproducibility of this form of standard.

Results

Simulated in vivo measurements of calcium in bones.— In this section, the results of the bone experiments, together with the relevant experimental parameters, are presented in tabular form. The results given for the femurs do not include final adjustments resulting from the differences in relative calcium concentration between the models and bone along the length of the samples. The sinusoidal sweeps that were used in these experiments operated in conjunction with these relative differences to bias the experiments. However, the subsequent definition of calcium content in various parts of the femur, knowledge that the models had constant concentration in all parts, and analysis of the residence time of each part in the beam and before the detector permitted computation of an appropriate correction for the bias. The final corrected values are given later.

The first femur experiments were merely exploratory. A femur bone and three models were sequentially irradiated for 10 min, as previously described, and then were counted for 10 min while sweeping back and forth in front of an aboveground 7.6-cm by 7.6-cm NaI(Tl) detector. The results are given in table 5, and the gamma-ray spectrum of the bone is shown in figure 3.

The second series of experiments was similar to the first. Femur bone and models were irradiated as before, and a second clamp held a vertebra (No. 1) bone or model for simultaneous irradiation. Corresponding models (e.g., femur model No. 4 and vertebra model No. 4) were irradiated together, as were the two kinds of bones. To avoid excessive background counting rates, these samples were counted in the underground bunker. A 12.7-cm by 12.7-cm NaI(Tl) detector was used to count the femur samples, and a 7.6-cm by 7.6-cm

NaI(Tl) detector was used to count the vertebra samples. Each irradiation time and each counting time was of 10-min duration. The results of the second series of experiments are summarized in table 6.

In the third series of experiments, the vertebra models and bone (vertebra No. 1) were sequentially irradiated for 10 min in a fixed position above the beam port while the reactor was operated at 250 kW. Flux-monitor foils were used. After irradiation, the samples were counted with the 12.7-cm by 12.7-cm NaI(Tl) detector while in a fixed position. The results are given in table 7, and the gamma-ray spectrum of the bone is shown in figure 4.

In the fourth series of experiments, a femur and two femur models were sequentially irradiated for 15 min apiece, and immediately after being irradiated, each sample was counted for 15 min with the 12.7-cm by 12.7-cm NaI(Tl) detector. The pendulum holder was used, with 12-in. sweeps, for the irradiations; and the piston holder was used, with 3-in. sweeps, for counting. The results of these experiments are given in table 8. The gamma-ray spectrum of the bone is shown in figure 5, where it can be seen that the 3.1-MeV photopeak of Ca^{49} is considerably improved over that from the preliminary experiment (fig. 3).

In the final series of experiments, the second vertebra (No. 2) and two vertebra models were sequentially irradiated for 10 min in a fixed position above the beam port while the reactor was operated at 250 kW. Flux-monitor foils were used. After irradiation, the samples were counted with the 12.7-cm by 12.7-cm NaI(Tl) detector while in a fixed position. The results are given in table 9.

Independent calcium assay in bones.— Neutron activation analysis and atomic absorption analysis were used to perform an independent calcium assay in bones.

Neutron activation analysis: The results of the neutron activation

analysis of vertebra No. 1 are given in table 10. The calcium content shown in the table was derived by comparison of Ca^{49} photopeak activity (3.1 MeV) with that of a calcium carbonate slurry in 1 ml of water. This standard was designed to simulate the geometry of the sample segments. Later experiments showed that this type of standard contributes an uncertainty of about 3.5% to the result owing to variability of slurry behavior.

The results of the neutron activation analysis of the femur and vertebra No. 2 are given in tables 11 and 12, respectively. In both cases, dry calcium carbonate was used as the comparator standard because the segments were specially cut to be evenly distributed in the vials.

The results of the comparison of dry calcium carbonate standards with calcium citrate are given in table 13, together with the results of the measurement of three standards prepared by slurrying $CaCO_3$ in 5 ml of water. It can be seen that the dry comparator standards agree to within about 0.5% of the average value. Hence, in the standard neutron activation analysis determinations, where dry $CaCO_3$ comparator standards were used, no adjustment of the values was necessary. However, in the case of vertebra No. 1, where uneven distributions of the specimen fragments in the vials were duplicated by slurried $CaCO_3$, the comparator standards have a poorer reproducibility. Therefore, it was necessary to include the ±3.5% relative standard deviation of the comparator value in the precision of the neutron activation analysis results.

Atomic absorption analysis: The atomic absorption analysis was performed by a separate group, the Analytical Group of the Gulf General Atomic Chemistry Department, and the results are completely independent of the neutron activation analysis results.

The three weighed sections of vertebra No. 1 were dissolved in hydrochloric acid, and then the solutions were made to an accurate volume and thoroughly mixed. Small aliquots of each solution were aspirated into the flame (total-consumption burner) of an atomic-absorption spectrophotometer,

and the percent transmission of the 4227-A light from a calcium hollow cathode lamp through the flame was measured. To obtain values of calcium concentration in the solutions, the results were compared with a calibration curve derived from measuring standard solutions of calcium in the same manner. The solution concentration values, in mg/ml, multiplied by the solution volume yielded the total calcium content in each part, as given in table 14. The second vertebra and the femur were similarly analyzed, and the results are given later in table 16.

Correction for sinusoidal sweep bias in femur analysis by in vivo neutron activation analysis.— A model of the femur was sectioned in the same manner as the bone and each part was weighed. The relative calcium activations to be expected from the bone and model were compared by computing the fraction of calcium in the various sections and multiplying by the fractional time the sections were exposed to the beam during a sinusoidal sweep. In these calculations, the fraction of calcium in each section of the model was taken to be directly proportional to the fraction of the total model weight in each section. Table 15 shows the results of the computation.

The relative activation of the model divided by that of the bone gives a ratio of 1.025. This is the factor by which the calcium values in the actual femur obtained by simulated in vivo neutron activation analysis must be multiplied to correct for the bias induced by sinusoidal sweeps during activation.

Whereas the irradiation geometry was sharply defined by a clear-cut 4-in.-diameter neutron beam, the counting geometry was such that all parts of the femur were counted during all parts of the sweep. Therefore, the sinusoidal sweep bias in counting proved to be comparatively insignificant.

Summary of fully corrected calcium determinations.— The weights of calcium in the bones analyzed by the various methods are summarized in table 16. These results are fully corrected for factors previously discussed. The preliminary femur experiment and the preliminary vertebra experiment are not included in the summary.

Neutron-flux characteristics.—

Cylinders: Results obtained from the irradiation of 2-dram, calcium-loaded cylinders are given in table 17. The sample configurations are as follows:

Sample No. 1 was a bare cylinder.

Sample No. 2 was a cylinder in a polyethylene vial.

Sample No. 3 was a cylinder in a polyethylene vial, and the bottom half of the vial (the end and side toward the neutron beam) was covered with 0.15 cm of paraffin.

Sample No. 4 was a cylinder in a polyethylene vial, and the bottom half of the vial was covered with 0.65 cm of paraffin.

Sample No. 5 was a cylinder in a polyethylene vial, and the top half of the vial (the ends and side away from the neutron beam) was covered with 0.15 cm of paraffin.

Sample No. 6 was a cylinder in a polyethylene vial, and the top half of the vial was covered with 0.65 cm of paraffin.

Sample No. 7 was a cylinder in a polyethylene vial, and the vial was completely covered with 0.15 cm of paraffin.

Sample No. 8 was a cylinder in a polyethylene vial, and the vial was completely covered with 0.65 cm of paraffin.

Discs: As previously described, the two stacks of discs were irradiated simultaneously in one experiment with each of five sequentially irradiated vertebrae (four models and one bone). The final irradiation ended at 11:15, and the counting rates of the 0.51-MeV photopeak of Cu^{64} in the copper foils

at the bottom of the vertebrae were corrected to that time with the appropriate decay factors. The counting rates of the 0.51-MeV Cu^{64} photopeaks of the copper flux monitors in each set of discs were also corrected to 11:15 with the appropriate decay factors. The corrected counting rates are given in table 18.

The results of the experiment where the stack of nylon discs was irradiated by itself for 15 min are given in table 19. These results have also been corrected with the appropriate decay factors. The marked effect of hydrogenous material on neutron flux that is evidenced by these experiments is discussed later.

Calcium and sodium.— For the solution containing 5 μg of sodium and 50 μg of calcium, the described procedure (10-min irradiation, 4-min delay, and 10-min count) produced the gamma-ray spectrum shown in figure 6. The integrated 2.75-MeV photopeak of Na^{24} and the integrated 3.1-MeV photopeak of Ca^{49} were each measured, and the following specific activities in the peaks at the end of the 10-min irradiation were computed:

Ca^{49} (3.1-MeV photopeak) . . 16.5 cpm/μg of calcium

Na^{24} (2.75-MeV photopeak) . . 124 cpm/μg of sodium

Cockroft-Walton generator experiments.— The 10-min irradiation of 10.5187 g of $CaCO_3$ with 1/8 in. of paraffin between the sample and the neutron source was accompanied by 589 463 counts on the BF_3 monitor. The 10-min irradiation of 14.1154 g of $CaCO_3$ with 3-1/2 in. of paraffin between sample and neutron source was accompanied by 1 139 485 counts on the BF_3 counter. Approximately 2 min after the end of each irradiation, the sample was measured for a live time of 10 min, with a 7.62-cm by 7.62-cm NaI(Tl) detector coupled to a multichannel pulse-height analyzer. In each case, the 3.1-MeV photopeak of 8.8-min Ca^{49} and the 1.15-MeV photopeak of 22-min K^{44} were observed in the resulting gamma-ray spectra. The photopeak counting rates of these two radionuclides permitted the computation of thermal- and fast-neutron fluxes at the sample position. These fluxes, and a description of the experimental conditions, are given in table 20.

The flux derived for fast neutrons is based on the $Ca^{44}(n,p)K^{44}$ reaction, which has an effective (nuclear plus coulomb barrier) threshold of 9.1 MeV. Since most 14-MeV neutrons that undergo a single scattering event in paraffin will be dropped to <9.1 MeV, the fast-neutron fluxes given in Table 20 are essentially 14-MeV neutron fluxes.

DISCUSSION

Experimental Results

The first determination of calcium in the femur and the first determination of calcium in the vertebra (No. 1) were of a preliminary nature, and in both cases the standard deviations of the final results (±12% of the value and ±19% of the value) reflect this fact. Therefore, the results of these experiments are not included in the following discussion. Application of realistic improvements quickly brought dramatic improvements, with relative standard deviations for calcium values in femur and vertebra dropping immediately to about ±3% and ±6%, respectively.

The total calcium in vertebra No. 1 was determined by three methods: 1.47±0.08 g by simulated in vivo neutron activation analysis, 1.47±0.02 g by standard neutron activation analysis, and 1.54±0.05 g by atomic absorption spectrophotometry. The statistical overlap of these three values, as defined by their respective standard deviations, indicates that the values are in very good agreement. It can be seen from the standard deviation of the simulated in vivo value that the agreement between this value and the standard neutron activation analysis value was fortuitous.

Similarly, the determination of calcium in the femur by simulated in vivo neutron activation analysis (an average of 8.21±0.31 g in two determinations, corrected for sweep bias) agreed very well with the value of 8.38±0.10 g obtained by standard neutron activation analysis. Finally, the calcium values

obtained for vertebra No. 2 by simulated in vivo neutron activation analysis and standard neutron activation analysis (1.52±0.10 and 1.67±0.02 g, respectively) were in fair agreement. The standard deviations were such that there is a 20% chance that the true value from the simulated in vivo neutron activation analysis experiment was $\geq$1.645 g of calcium, and a 20% chance that the true value from the standard neutron activation analysis experiment was $\leq$1.645 g of calcium. The average of all values (Table 16) are given in the summary.

The mode of irradiating the vertebrae, wherein a specimen was over the beam port during the power rise of the reactor, necessitated the use of flux monitors, since it was not possible to bring the reactor to power in an exactly reproducible fashion. However, the femurs were not brought into the beam until after the reactor was at full power, and since the reactor is servo-controlled to maintain an accurate power level, flux monitors were not required.

The experiments pertaining to the effect of hydrogenous material on the thermal-neutron flux within the sample give striking evidence that size and configuration critically influence the flux. In the experiments with calcium-loaded cylinders, the effect of the thicker paraffin cover was very strong. When the paraffin was interposed between the neutron beam and the sample, the flux at the sample was only ~62% of that when the paraffin was absent, and when the paraffin was only on the opposite side of the sample, the flux was ~141% of that when the paraffin was absent. Furthermore, these opposite effects cancelled each other when the paraffin completely covered the sample. The need for comparator standards that faithfully match the dimensions and configurations of the specimen for in vivo neutron activation analysis estimation of bone calcium was clearly brought out by these experiments.

The disc experiments provide additional evidence regarding the influence of size and shape and demonstrate the presence of a "buildup" of neutron flux as a result of scattering. The buildup is clearly seen in the nylon-disc data and is easily demonstrated in the case of the measurements on smaller polyethylene discs.

The macroscopic scattering cross section of polyethylene is calculated, from a hydrogen concentration of 8.1×10^{22} atoms/cc and a microscopic scattering cross section of 3.5×10^{-23} cm^2/atom, to be 2.84/cm. However, while the flux attenuation with distance as a result of scattering losses might be given by $e^{-(2.84)(x)}$ (where x is the penetration distance) in a sample of very small diameter, the flux in the 7/8-in. polyethylene discs was attenuated in accordance with $e^{-(1.33)(x)}$. This variation in flux attenuation with sample size is as follows:

Polyethylene thickness, x	$e^{-(2.84)(x)}$	$e^{-(1.33)(x)}$	Relative experimental flux (7/8-in. discs)[a]
0	1.0	1.0	1.0
0.5	0.24	0.51	0.56
1.0	0.058	0.26	0.27
1.5	0.014	0.14	0.14
2.0	0.0034	0.070	0.064
2.5	0.00080	0.036	0.036
3.0	0.00020	0.019	0.019
3.5	0.000045	0.0096	0.010

[a] See table 18.

If the effective buildup factor is defined as the ratio between the macroscopic cross section of hydrogen (2.84) and the applicable substitute value (1.33), then the buildup factor is 2.14. However, the fact that this buildup factor is reasonably constant throughout the 3.5-cm polyethylene discs represents a fortuitous balance between the various relevant processes (contributory scattering, scattering losses, and thermalization of epithermal neutrons). No such balance existed in the nylon-disc experiments.

The relative effect of contributory neutron scattering (plus thermalization) over scattering losses was much greater in the case of the 3-in.-diameter nylon discs than it was for the 7/8-in.-diameter polyethylene discs. This effect is so strong that the thermal-neutron flux is greater

at penetration depths of 0.5 cm and 1.0 cm than at the face of the assembly (zero penetration). Indeed, this effect was so pronounced that the experiment was performed twice to make sure the results were valid.

The data from the Cockroft-Walton generator experiments showed that an excessive fast-neutron flux is present along with the useful thermal-neutron flux. The fast-neutron flux values given here, which were measured with a reaction requiring neutrons with energies >9 MeV, do not include the fluxes of neutrons having energies between thermal energy and 9 MeV. Thus, the fast-neutron dose rates at the sample that were computed from the generated K^{44} activity--about 4×10^4 rem/hr with 1/8 in. of paraffin between the source and the sample, and about 1×10^3 rem/hr with 3-1/2 in. of paraffin between the source and the sample*--are understatements of the true fast-neutron dose rates. Such radiation dose rates should not be used for the time necessary to generate a useful amount of Ca^{49} in in vivo work. The reactor beam is much safer in this regard.

The nuclear reactor neutron beam used in simulated in vivo experiments was derived from the top of the graphite reflector surrounding the TRIGA Mark I reactor core. The neutron energy spectrum at the reflector position has been described by West (ref. 23). With the thermal-neutron flux values taken as unity, the more energetic components of the beam have the following relative fluxes and (again utilizing Federal Register values to compute doses) relative dose rates:

*Obtained by dividing the flux values (n/cm^2-sec) given in table 20 by the number of 14-MeV neutrons/cm^2 specified in the Federal Register (Title 10, Part 20) to deliver 1 rem, and multiplying by 3600 sec/hr.

Energy	Relative flux	Relative dose rate
Thermal	1	1
>thermal and <100 eV	0.1	0.136
100 eV - 5 keV	0.067	0.080
5 keV - 20 keV	0.055	0.132
20 keV - 100 keV	0.027	0.220
100 keV - 500 keV	0.014	0.315
500 keV - 1 MeV	0.0084	0.317
1 MeV - 2.5 MeV	0.0033	0.110
2.5 MeV - 5 MeV	0.0016	0.060
5 MeV - 7.5 MeV	0.0005	0.020
7.5 MeV - 10 MeV	0.0001	0.004

From the above values, it can be seen that the epithermal- plus fast-neutron dose from the beam was only ∿1.4 greater than the thermal-neutron dose, and that the total flux of epithermal plus fast neutrons was ∿0.28 of the thermal-neutron flux. With the thermal-neutron flux equal to 2×10^6 n/cm^2-sec in the sample position, a time of 485 sec was required to deliver 1 rem of thermal neutrons; i.e., the thermal-neutron dose rate to the sample was 7.5 rem/hr. The epithermal- and fast-neutron dose rate was 11 rem/hr; thus, the total neutron dose rate was 18.5 rem/hr. In the 10-min irradiations utilized in most of the experiments, the maximum delivered neutron dose was 3.1 rem, and an equivalent dose of gamma rays was delivered.

The contrast between the doses delivered by a 14-MeV neutron source and those delivered by a reactor beam port showed the latter to be the more suitable tool for this work.

Finally, it was shown that no serious interference with the in vivo determination of calcium by neutron activation analysis is to be expected from sodium in the body.

Prospects for Actual In Vivo Determination of Bone Calcium by Neutron Activation Analysis

As shown in table 1, 1.4×10^8 net photopeak (3.1 MeV) cpm is obtained

with a 7.6-cm by 7.6-cm NaI(Tl) detector subsequent to the irradiation of 1 g of calcium for 1 hr in a thermal-neutron flux of 3.5×10^{12} n/cm^2-sec. From this, one can compute that a biologically safe, 10-min irradiation in a thermal-neutron flux of 2×10^6 n/cm^2-sec would enable an investigator to obtain 436 net photopeak cpm per gram of calcium with the same detector. Allowing for a baseline contribution of about 20% of the net counts, one would expect a relative standard deviation of ∿5%, based on counting statistics only, in a 1-min count. Similarly, the relative standard deviations subsequent to safe irradiation of 1.5 g (monkey vertebra) and 8.2 g (monkey femur) of calcium would be about ±4% and ±2%, respectively.

In practice, of course, a comparator standard is used, and since the comparator standard must have essentially the same composition and form as the sample, similar relative standard deviations, based on counting statistics, would be obtained. Thus, with 1-min counts, the overall counting statistics in the determination of calcium in the vertebra and femur would be about ±6% and ±3%, respectively.

In the present work, general counting geometries (particularly in the case of the femur) were considerably poorer than those cited in the above discussion. However, this factor was offset to some extent by the use of longer counting periods and the larger, 12.6-cm by 12.6-cm, detector, and the counting precisions obtained (vertebra, ±6% relative; femur, ±4% relative) were nearly as good as those estimated above. The experimental work therefore suggests that reasonable estimates of attainable precisions can be made for other bone weights. Such estimates have been made on the basis that comparatively inefficient single-detector counting geometries of larger samples can be compensated for by using longer counting periods and an array of detectors. These estimates are given in table 21.

It has been experimentally demonstrated that the estimates given in table 21 for bone samples of up to 30 g are well within the reach of practical achievement. However, although overall relative standard deviations of about ±1% might be achieved in serial measurements involving two measurements each

of specimen and standard, it is doubtful that standards can be obtained that will permit the determination of calcium with absolute accuracies and precisions of better than 2% to 3% for any sample.

Assuming that a precision of 1% is attainable in the serial measurement of whole-body calcium losses of a given monkey having a total of 300 g of body calcium, there is less than a 50% chance that a change of 2 g or less of calcium could be detected. The chances for detecting, with serial measurements, changes of more than 2 g out of 300 g of calcium are as follows (in each case, the precision and accuracy of the measurement are about ±3 g):

Change in calcium, g	Probability of detection,%
2.4	57
3	68.3
4	82
4.8	94.6
6	97.6
7.2	98.4

In general, it is expected that the demonstrated accuracy for the measurement of calcium in the femur will be realized in actual in vivo measurements of the femur, humerus, spinal column, and tibia. Therefore, providing changes in bone density are directly proportional to changes in calcium, changes in density of 5%, 10%, 15%, and 20% in these bones should be measurable with accuracies (given as percentage of the change) of 60%, 30%, 20%, and 15%, respectively. That is, where a standard deviation of about ±0.18 g Ca is obtained in the measurement of bones containing around 6 g of Ca (see table 21), the standard deviation is about 60%, 30%, 20%, and 15%, respectively, of 0.3-, 0.6-, 0.9-, and 1.2-g changes of total calcium content. A precision of ±4% to ±5% of the value is expected in the measurement of calcium in the os calcis. Hence, 5%, 10%, 15%, and 20% changes would

be measured to the nearest 100%, 50%, 33%, and 25% of the value of the change, respectively.

The precision with which calcium in the pelvis can be measured is somewhat uncertain at this time because of the presence of adjacent bones that would become simultaneously activated (femur and/or sacrum). It should be possible to confine most of the activation to the ilium, in which case serial measurement may be able to determine changes with the same order of accuracy as in the case of the femur.

The achievement of a comparator standard that is suitable for absolute calcium determination by in vivo neutron activation analysis should be fairly straightforward. It is suggested that two frozen monkeys first be compared by neutron activation analysis, and then stripped and prepared as articulated skeletons. The skeletons could then be compared by neutron activation analysis, after which one would be analyzed for calcium in detail by high-flux neutron activation analysis or atomic absorption spectrophotometry. Finally, the intact skeleton would be covered with tissue-equivalent material to conform to the original shape of the monkey. A standard prepared in this fashion would be durable, flexible, and fully characterized. This standard would be useful in measuring bone calcium in the whole body, or selected parts, of a live monkey on either an absolute or relative basis.

A large neutron port can be constructed at a nuclear reactor to allow the safe irradiation of a whole monkey. The port can be equipped with an adjustable shutter to allow portions of the monkey to be irradiated. The irradiated monkey can then be counted with a coupled array of large (12.6-cm by 12.6-cm) NaI(Tl) detectors in an underground room. With expanded versions of the comparator standard, beam port, and counting station, essentially the same procedure that was used in the present work can be applied to live monkeys.

In conclusion, it appears that the in vivo neutron activation analysis method can be developed to provide useful measurements of calcium in the macaque monkey.

Gulf General Atomic Incorporated
San Diego, California, June 13, 1969

REFERENCES

1. Lukens, H. R., Jr.: Estimated Photopeak Specific Activities in Reactor Irradiations, USAEC Report GA-5073 (Excerpt) (AT(04-3)-167), General Dynamics Corporation, General Atomic Division, September 9, 1964.
2. Hughes, D. J.; and Schwartz, R. B.: Nuclear Cross Sections. USAEC Report BNL-325, Second ed., Brookhaven National Laboratory, July 1958.
3. Roy, J. C.; and Hawton, J. J.: Table of Estimated Cross Sections for (n,p), (n,α) and (n,2n) Reactions in a Fission Neutron Spectrum. Report No. AECL-1181, Atomic Energy of Canada Ltd., December 1960.
4. Heath, R. L.: Scintillation Spectrometry — Gamma-Ray Spectrum Catalogue. USAEC Report IDO-16408 (AT(10-1)-205), Phillips Petroleum Company, Atomic Energy Division, July 1957.
5. Strominger, D.; Hollander, J. M.; and Seaborg, G. T.: Table of Isotopes. Rev. Mod. Phys., vol. 30, no. 2, Apr. 1958, pp. 585-904.
6. Kenna, B. T.; and Conrad, F. J.: Tabulation of Cross Sections, Q-Values, and Sensitivies for Nuclear Reactions of Nuclides with 14-Mev Neutrons. USAEC Report SC-RR-66-229 (AT(29-1)-789), Sandia Corporation, June 1966.
7. Glasstone, S., ed.: The Effects of Atomic Weapons. Revised ed., U.S. Government Printing Office, 1950, p. 342.
8. Federal Register, Title 10, Part 20, November 17, 1960. U.S. Government Printing Office.
9. Hawk, P. B.; Oser, B. L.; and Summerson, W. H.: Practical Physiological Chemistry. The Blakiston Co., New York, 1951.

10. Soremark, R.; and Bergman, B.: Gamma Ray Spectrometric Analysis of Some Microelements in Human Mandibular Compact Bone. Acta Isotopica, vol. 2, no. 5, 1962, pp. 5-19.

11. Maletskos, C. J.; Osborn, H. F.; and Braun, A. G.: In Vivo Bone Calcium Determinations, in Radium and Mesothorium Poisoning and Dosimetry and Instrumentation Techniques in Applied Radioactivity. USAEC Report NYO-9505 (AT(30-1)-952), pp. 47-49.

12. Anderson, J.; Osborn, S. B.; Tomlinson, R. W. S.; Newton, D.; Rondo, J.; Salmon, L.; and Smith, J. W.: Neutron Activation Analysis in Man In Vivo. Lancet, vol. 2, Dec. 1964, pp. 1201-1205.

13. Lenihan, J. M. A.: Activation Analysis. Nature, vol. 207, Jul. 1965, pp. 347-349.

14. Lenihan, J. M. A.; Comar, D.; Riviere, R.; and Kellershohn, C.: Estimation of Thyroid Iodine in vivo by Activation Analysis. Nature, vol. 214, Jun. 1967, pp. 1221-1223.

15. Battye, C. K.; Tomlinson, R. W. S.; Anderson, J.; and Osborn, S. B.: Experiments Relating to Whole-Body Activation Analysis in Man In Vivo Using 14-MeV Incident Neutrons, in Nuclear Activation Techniques in the Life Sciences, Proceedings of a Symposium, Amsterdam, 8-12 May 1967. International Atomic Energy Agency, Vienna, 1967, pp. 573-582.

16. Boddy, K.; and Alexander, W. D.: Clinical Experience of In Vivo Activation Analysis of Iodine in the Tyroid Gland, in Nuclear Activation Techniques in the Life Sciences, Proceedings of a Symposium, Amsterdam, 8-12 May 1967. International Atomic Energy Agency, Vienna, 1967, pp. 583-597.

17. Palmer, H.E.; Nelp, W. B.; Murano, R.; and Rich, C. R.: Measurement of Total Body Calcium (Skeletal Mass) in Man by In Vivo Neutron Activation Analysis and Total Body Counting. J. Nucl. Med., vol. 8, 1967, p. 268.

18. Palmer, H. E.; Nelp, W. B.; Murano, R.; and Rich, C.: The Feasibility of In Vivo Neutron Activation Analysis of Total Body Calcium and Other Elements of Body Composition. Phys. Med. Biol., vol. 13, no. 2, 1968, pp. 269-279.

19. Comar, D.; Crouzel, C.; Chasteland, M.; Riviere, R.; and Kellershohn, C.: The Use of Neutron-Capture Gamma Radiation for the Analysis of Biological Samples. Nucl. Appl., vol. 6, no. 4, Apr. 1969, pp. 344-351.

20. Comar, D.; Riviere, R.; Raynaud, C.; and Kellershohn, C.: Recherches Preliminaries sur la Composition et le Metabolisme de l'os Etudies par Radioactivation Neutronique in vivo chez l'Homme, in Radioisotopes in Klinik und Forschung. Vol. VIII. Urban & Schwarzenberg (Munich), 1968, p. 186.

21. Fairchild, R. G.: Development and Dosimetry of an Epithermal Neutron Beam for Possible Use in Neutron Capture Therapy. I. Epithermal Neutron Beam Development. Phys. Med. Biol., vol. 10, 1965, pp. 491-504.

22. Anon.: Measurements in the Body. Nature, vol. 222, Apr. 26, 1969, p. 325.

23. West, G. B.: Calculated Fluxes and Cross Sections for TRIGA Reactors. Report No. GA-4361, General Dynamics Corporation, General Atomic Division, August 14, 1963.

TABLE 1

Photopeak Counting Rates of Calcium

Radionuclides Produced in Reactor Irradiations

Target Isotope	Reaction	Product Radionuclide	Half Life	Gamma Ray Energy (Mev) [a]	Photopeak Counts Per Minute Per Gram of Calcium
Ca^{40}	(n, 2n)	Ca^{39}	1 s	0.51	9.2×10^4
Ca^{42}	(n, p)	K^{42}	12.5 h	1.53	1.6×10^4
Ca^{43}	(n, p)	K^{43}	22.4 h	0.61	3.6×10^4
Ca^{44}	(n, p)	K^{44}	22 m	1.13	1×10^5
	(n, α)	Ar^{41}	1.8 h	1.29	6.0×10^1
Ca^{46}	(n, γ)	Ca^{47}	4.7 d	1.31	7.0×10^3
Ca^{48}	(n, γ)	Ca^{49}	8.8 m	3.10	1.4×10^8
	(n, 2n)	Ca^{47}	4.7 d	1.31	3.3×10^2

a) Only the most useful gamma ray is given. Several of these radionuclides emit gamma rays of more than one energy. For example, Ca^{49} emits 3.10 Mev gamma rays in 89% of its disintegrations and 4.1 Mev gamma rays in 10% of its disintegrations.

TABLE 2

Integrated Neutron Fluxes
to Deliver One Rem

Neutron Energy	Neutrons/cm^2 to Deliver One Rem	Neutron Energy	Neutrons/cm^2 to Deliver One Rem
Thermal	970×10^6	1 Mev	26×10^6
100 ev	720	2.5 Mev	29
5 kev	820	5 Mev	26
20 kev	400	7.5 Mev	24
100 kev	120	10 Mev	24
500 kev	43	10 - 30 Mev	14

TABLE 3

Specific Activities of the Most Significant Radionuclides Produced by a 10 Minute Irradiation of the Body at a Thermal Neutron Flux of 3.5×10^6 n/cm^2-sec

Element	Avg. Body Abundance,[a] %	Radionuclide Product Species	Half Life	Energy of Gamma Ray, Mev	Specific Activity,[b] Photopeak cpm per Gram of Body Tissue
Na	0.15	Na^{24}	15 h	1.37	1.7
				2.75	0.8
Mg	0.05	Mg^{27}	9.5m	0.84	0.3
				1.01	0.1
Cl	0.15	Cl^{38}	37.3m	1.60	1.5
				2.17	1.4
K	0.35	K^{42}	12.5h	1.52	0.06
Ca	1.5	Ca^{49}	8.8m	3.10	1.2
				4.10	0.1
S	0.25	S^{37}	5.0m	3.09	0.0032

a) Abundances in the human adult. The macaque monkey may be expected to have relatively more calcium than the human adult.

b) Computed as specified in ref. 1, with allowance for body concentrations.

TABLE 4

Models

Model	Weight, g	Ca,%	Ca, g
Femur No. 1	39.2126	7.49	2.9368
" 2	40.3156	9.80	3.6611
" 3	40.4704	10.80	4.3708
" 4	42.1301	16.0	6.7408
" 5	30.8969	26.2	8.0952
Vertebra No. 1	8.5620	7.49	0.6413
" 2	8.4856	9.80	0.8316
" 3	8.4946	10.80	0.9174
" 4	7.7172	16.0	1.2348
" 5	7.3713	26.2	1.9313

TABLE 5

First Femur Experiments

(10 Min. Irradiations, 10 Min. Counts, Both with Sinusoidal Sweeps)

Femur Sample	Timing[a] End of Irradiation	Start of Count	End of Count[b]	Decay Factor[c]	3.1 Mev Photopeak Counts, Ca^{49}, Observed Gross	Baseline	Net	Model, Counts per Gram Ca[d]	Apparent Calcium in Bone, Grams[e]
Model 1	34.50	37.30	47.40	0.585	776	566	210	121	
" 2	49.52	51.50	61.60	0.576	789	569	220	97	
" 3	64.43	66.10	76.19	0.590	1102	816	286	108	
Bone	79.40	81.10	91.15	0.588	523	94	429		6.70 ± 0.82
							Avg.	109 ± 12	

a) Referred to an electric timer that was started prior to the experiments.

b) The elapsed time is slightly in excess of instrument live time.

c) Fraction of activity at the end of the irradiation that remained at the midpoint of the counting period.

d) Corrected to the end of the irradiation.

e) Net bone counts, corrected to the end of the irradiation, divided by the average counts per gram of Ca. Not corrected for sinusoidal sweep effects.

TABLE 6

Combination Femur and Vertebra (No. 1) Experiments

(10 Min. Irradiations, 10 Min. Counts, Both with Sinusoidal Sweeps)

Sample	Timing[a]			3.1 Mev Photopeak Counts Ca^{49}, Observed			Model, Counts Per Gram Ca[d]	Apparent Calcium in Bone, Grams[e]
	End of Irradiation	Start of Count	End of Count[b]	Decay Factor[c]	Gross	Baseline	Net		
Femur Model 4	11.50	13.75	23.99	0.560	4309	742	3562	944	
Femur Model 3	25.50	27.40	37.63	0.576	2985	539	2446	939	
Femur Model 1	39.80	41.30	51.53	0.594	2045	406	1639	938	
Femur	62.30	64.10	74.36	0.580	5440	1134	4306		7.91 ± 0.15
						Model Femur Avg.		940 ± 5	
Vertebra Model 4	11.50	14.25	24.26	0.538	297	116	181	273	
Vertebra Model 3	25.50	27.80	37.81	0.558	256	80	176	344	
Vertebra Model 1	39.80	42.00	52.01	0.563	150	56	94	260	
Vertebra	62.30	64.40	74.41	0.566	338	112	226		1.37. ± 0.26
						Model Vertebra Avg.		292 ± 48	

a) Referred to an electric timer that was started prior to the experiments.

b) The elapsed time is slightly in excess of the instrument live time.

c) Fraction of activity at the end of the irradiation that remained at the midpoint of the counting period.

d) Corrected to the end of the irradiation.

e) Net bone counts, corrected to the end of the irradiation, divided by the average counts per gram of Ca. Not corrected for sinusoidal sweep effects.

TABLE 7

Vertebra Experiments (Vertebra No. 1)

(Third Series of Experiments)

(Irradiation and Counting in Fixed Position)[a]

Sample	Timing[b] End of Irradiation	Start of Count	End of Count[c]	Decay Factor[d]	Photopeak Counts, Observed, 3.1 Mev in Bone & Models, 0.51 Mev in Flux Monitors: Gross	Baseline	Net	At End of Irradiation: Flux Monitor, Counts per Gram Copper[e]	Model Counts per Gram Ca[f]	Apparent Calcium in Bone, g[g]
Model 1	12.77	14.75	25.06	0.574	1873	360	1513		4115	
76.5 mg Monitor on "	12.77	273	277	0.790	4994	962	4032	66,700		
Model 3	27.06	28.75	39.07	0.585	2870	600	2270		4230	
72.3 mg Monitor on "	27.06	291	295	0.788	4490	770	3720	65,300		
Model 4	40.86	42.50	52.83	0.585	4063	840	3223		4450	
73.6 mg Monitor on "	40.86	298	302	0.789	4309	444	3865	66,900		
Model 5	54.42	56.05	66.39	0.586	5934	1125	4809		4250	
71.5 mg Monitor on "	54.42	313	317	0.790	4166	420	3746	66,300		
Bone	68.10	69.70	80.05	0.586	4135	960	3175			1.47 ± 0.08
75.9 mg Monitor on "	68.10	324	328	0.791	3914	432	3482	57,900[h]		

a) 10 min. irrad., bone and models counted 10 min., monitors counted 4 min.

b) Referred to an electric timer that was started prior to the experiments.

c) The elapsed time is slightly longer than instrument live time.

d) Fraction of activity at end of irradiation remaining at midpoint of the counting period.

e) Corrected to the end of the irradiation. Model monitors avg. 66, 300 ± 720 c/g.

f) Avg. value is 4261. Values are corrected to end of irradiation.

g) $\frac{(\text{Net counts, bone})(\text{model monitor/bone monitor ratio})}{(\text{bone decay factor})(\text{avg. model counts per gram Ca})} = \frac{(3175)(1.15)}{(0.586)(4261)} = 1.47.$

h) Avg. model monitor counts to bone monitor count ratio is 1.15.

TABLE 8

Femur Experiments

(15 Min. Irradiations, 15 Minute Counts[a], Both with Sinusoidal Sweeps)

Sample	Timing[b] End of Irradiation	Start of Count	End of Count	Decay Factor[c]	3.1 Mev Photopeak Counts, Ca^{49}, Observed Gross	Baseline	Net	Model, Counts Per Gram Ca[d]	Apparent Calcium in Bone, Grams[e]
Model 4	20.54	23.00	38.00	0.458	6808	1232	5576	1800	
Model 5	44.90	46.80	61.80	0.476	8074	1568	6506	1690	
Bone	67.00	69.80	84.80	0.444	8185	1904	6281		8.10 ± 0.29

a) Elapsed time. Live times were: Model 4 = 14.65 min., Model 5 = 14.65 min., bone = 14.65 min.

b) By electric timer.

c) Fraction of original activity remaining at midpoint of count.

d) Corrected to end of irradiation.

e) Net bone counts, corrected to end of irradiation, divided by average counts per gram of Ca (1745). Not corrected for sinusoidal sweep factor.

TABLE 9

Vertebra Experiments (Vertebra No. 2)

(Irradiation and Counting in Fixed Positions)[a]

Sample	Timing[b] End of Irradiation	Start of Count	End of Count[c]	Decay Factor[d]	Photopeak Counts Observed, 3.1 Mev in Bone & Models 0.51 Mev in Flux Monitors Gross	Baseline	Net	At End of Irradiation Counts per Gram Copper[e]	Counts per Gram Ca[f]	Apparent Calcium in Bone,[g]
Model 4	20.09	21.77	32.11	0.582	3950	816	3134		4380	
72.7 mg Monitor on "	20.09	165	175	0.877	11935	2100	9835	154,000		
Bone	34.33	36.04	46.37	0.580	4036	952	3084			1.52 ± 0.10
76.6 mg Monitor on "	34.33	177	187	0.879	10123	2000	8123	121,000[h]		
Model 5	49.68	51.22	61.56	0.589	5805	1236	4569		4020	
76.1 mg Monitor on "	49.68	190	200	0.881	11205	2150	9055	135,000		

a) 10 Min. Irrad.; Bone, Models, and Monitors Counted for 10 min. (Live time.)

b) Referred to electric timer.

c) The elapsed time for counting bone and models is slightly longer than instrument live time.

d) Fraction of original activity remaining at midpoint of count.

e) Corrected to end of irradiation. Model monitors avg. 144,500 ± 9,500.

f) Corrected to end of irradiation. Avg. value is 4200.

g) $\frac{\text{(Net counts, bone) (ratio, model monitor/bone monitor)}}{\text{(bone decay factor) (Avg. model counts per gram Ca)}} = \frac{(3084)(1.20)}{(0.580)(4200)} = 1.52.$

h) Avg. model monitor to bone monitor ratio is 1.20.

TABLE 10

Analysis of Vertebra No. 1 by NAA

Sample[a]	Timing[b] Irradiation, Seconds	Start of Count, min.	End of Count, min.	Live Count Time	Decay Factor	3.1 Mev Photopeak, Net Counts per Minute, Observed	Standard, Counts per Minute per Gram Ca [c]	Apparent Bone, Grams of Calcium [d]
1. Central processes	55.17	8.40	10.99	2 min.	0.468	13,298		0.531+0.066
2. Lateral processes and posterior hand bone	54.93	9.62	12.19	2 min.	0.424	11,858		0.523+0.064
3. Spongy bone and balance of hand bone	55.23	10.46	14.02	3 min.	0.381	8,558		0.420+0.052
4. Standard	54.93	9.73	14.31	4 min.	0.388	8,960	53,500	
							Total Ca	1.474+0.018

a) Weights in grams: No. 1 = 2.7340; No. 2 = 2.7578; No. 3 = 2.3705; No. 4 = 0.4312 g Ca as $CaCO_3$ slurry in 5 ml of water.

b) All Start and End of Count times are minutes after the end of the irradiation.

c) Corrected to the end of the irradiation.

d) (Sample, net cpm, obs.)/(decay factor)(cpm/g Ca) = Ca, grams in sample.

TABLE 11

Analysis of Femur by NAA

	Sample[a]	Timing: Irradiation, Seconds	Timing: End of Irrad to Midpoint of Count, min.	Timing: Count Live Time, min.	Timing: Decay Factor	3.1 Mev Photopeak, Net Counts per Minute, Observed	Standard, Counts per Minute per Gram Ca[b]	Apparent Grams of Calcium in Bone[c]
1.	Greater Trochanter	56.66	9.46	1.00	0.474	13,954		0.5156
2.	Head	56.44	11.65	1.00	0.400	13,228		0.5792
3.	Neck and Lesser Trochanter	56.42	13.00	1.00	0.360	14,994		1.1963
4.	Shaft	56.34	17.62	1.00	0.250	17,044		1.9582
5.	Shaft	56.54	17.46	1.00	0.254	14,257		1.6122
6.	Shaft	56.41	16.23	1.00	0.278	12,444		1.2857
7.	Medial Concyle	56.56	12.33	1.00	0.378	13,094		0.6106
8.	Lateral Condyle	56.48	12.92	1.00	0.362	12,839		0.6251
9.	Standard A	56.76	24.26	1.00	0.148	15,262	57,092	
							Total Bone Ca	8.38 ± 0.10

a) Weights (grams): No. 1 - 2.5164; No. 2 - 2.6939; No. 3 - 5.0581; No. 4 - 8.4260; No. 5 - 7.0634; No. 6 - 5.6714; No. 7 - 3.0137; No. 8 - 3.3848; No. 9 - 1.80624 g Ca as dry $CaCO_3$.

Lengths of femur: Total = 20.2 cm, samples 1, 2, 3 comprised 3.8 cm, sample 4 - next 4.6 cm, sample 5 - next 4.6 cm, sample 6 - next 4.2 cm, and samples 7 and 8 - final 3.0 cm.

b) Corrected to end of irradiation.

c) Based on standard A.

TABLE 12

Analysis of Vertebra No. 2 by NAA

Sample[a]	Irradiation, Seconds	End of Irradiation to Midpoint of Count, min.	Count Live Time Min.	Decay Factor	3.1 Mev Photopeak, Net Counts per Minute, Observed	Standard, Counts per Minute per Gram Ca[b]	Bone, Apparent Grams of Calcium
1. Processes	56.64	15.29	1.00	0.300	13,096		0.7694
2. Body, hard bone	56.43	6.38	1.00	0.606	15,706		0.4568
3. Body, spongy bone	56.15	5.93	1.00	0.627	15,846		0.4427
4. Standard	56.76	24.26	1.00	0.148	15,262	57,092	
						Total Bone Ca	1.67 ± 0.02

a) Weights (grams): No. 1 - 3.5011; No. 2 - 2.0560; No. 3 - 1.8834; Standard - 1.80624 g Ca as dry $CaCO_3$.

b) Corrected to end of irradiation.

TABLE 13

Comparator Standards

(5 ml. Volumes)

A. Dry Standards

Standard	Ca, g	3.1 Mev Photopeak, Net CPM at End of Irradiation	Net Peak CPM per Gram of Ca at End of Irradiation	Average Peak Activity, CPM/g Ca, at End of Irradiation
Ca Citrate	0.78589	47,041	59,857	
Ca Citrate	0.80418	47,889	59,550	59,704 ± 216
Ca Carbonate	1.7756	105,596	59,471	
Ca Carbonate	1.8549	112,545	60,674	60,073 ± 850

B. Slurries in 5 ml H_2O

Ca Carbonate	0.4114	28,965	70,406	
Ca Carbonate	0.4004	27,508	68,701	
Ca Carbonate	0.4086	30,081	73,620	70,909 ± 2500

TABLE 14

Atomic Absorption Analysis of Vertebra No. 1

Portion	Calcium, g
Central Processes	0.537±0.014
Lateral Processes and Posterior Hard Bone	0.539±0.014
Spongy Bone and Balance of Hard Bone	0.463±0.012
Total	1.539±0.048

TABLE 15

Relative Activation of Femur Sections, Bone and Model

Section	Overall Length, cm (sequential)	A, Fraction of Time in Beam During Sinusoidal Sweep	Bone		Model	
			B, Fraction of Total Calcium	Relative Activity, AxB	B, Fraction of Total Calcium	Relative Activity, AxB
1. Greater Trochanter, Lesser Trochanter, Head, and Neck	3.8	0.274	0.274	0.0750	0.289	0.0791
2. Shaft	4.6	0.234	0.234	0.0547	0.154	0.0360
3. Shaft	4.6	0.220	0.193	0.0425	0.159	0.0350
4. Shaft	4.2	0.237	0.153	0.0362	0.136	0.0322
5. Condyles	3.0	0.282	0.147	0.0415	0.262	0.0738
Total	20.2			0.2499		0.2561

TABLE 16

Calcium in Bones, Fully Corrected, Summary

Sample	Calcium, grams		
	Simulated In Vivo NAA	Standard NAA	Atomic Absorption
Vertebra No. 1	1.47 ± 0.08	1.47 ± 0.05	1.54 ± 0.05
Vertebra No. 2	1.52 ± 0.10	1.67 ± 0.02	1.58 ± 0.05
Femur Avg.	8.21 ± 0.31	8.38 ± 0.10	8.20 ± 0.20

TABLE 17

Cylinder Irradiations

(All Irradiations for 12 Minutes, Samples Counted for 4 Minutes)

Sample	Wt. of Cylinder, g.	Observed Net Count Rate, counts per minute	Decay Factor	Flux Monitor Factor	Counts Per Minute per Gram of Cylinder, Corrected for Decay & Flux
1	10.5221	177 ± 8	0.714	0.979	24.0 ± 1.1
2	10.6701	136 ± 8	0.486	0.979	26.6 ± 1.6
3	10.2445	182 ± 8	0.706	1.057	23.7 ± 1.0
4	10.3107	87 ± 7	0.480	1.057	16.6 ± 1.3
5	10.4585	193 ± 8	0.692	1.100	24.6 ± 1.0
6	10.3761	202 ± 10	0.475	1.100	37.4 ± 1.8
7	10.2291	164 ± 8	0.692	1.070	21.7 ± 1.1
8	10.1227	105 ± 4	0.373	1.070	26.1 ± 0.9

TABLE 18

Disc Experiments

Flux Monitor Position[a]	Specific Activity in 0.51 Mev Cu^{64} Photopeak of Flux Monitor, Counts per Minute per Milligram of Copper At the End of the Irradiation
Bottom of vertebra No. 1	18.2
" " " No. 2	14.9
" " " No. 3	16.3
" " " No. 4	16.4
" " " No. 5	14.5
(Integrated Vertebrae Foil Specific Activity)	80.3
Top of polyethylene disc No. 1	45.0
" " " " No. 2	22.1
" " " " No. 3	10.8
" " " " No. 4	5.1
" " " " No. 5	2.85
" " " " No. 6	1.55
" " " " No. 7	0.83
Bottom of nylon disc No. 1	41.7
Top " " " No. 1	56.9
" " " " No. 2	43.9
" " " " No. 3	33.8
" " " " No. 4	24.5
" " " " No. 5	13.7
" " " " No. 6	3.8

a) Disc position notation: Disc No. 1 is closest to the incident beam, disc No. 2 is adjacent to disc No. 1, etc.

TABLE 19

Nylon Disc Experiment

Disc No., Foil Position	Foil Activity, Photopeak (Cu^{64}) cpm/mg Cu at End of Irradiation	
	Centered Foil	Offset Foil[a)]
1, bottom	38.35	35.73
1, top	49.57	41.32
2, "	41.18	34.86
3, "	29.78	21.02
4, "	24.14	12.52
5, "	12.59	
6, "	3.12	

a) Placed at 2.68 cm from center of nylon disc to center of foil.

TABLE 20

Cockcroft-Walton Generator Experiments

	Paraffin Thickness Between Source & Sample	
	0.125 inch	3.5 inches
$CaCO_3$ weight, g	10.5187	14.1154
Irradiation time, minutes	10.00	10.00
BF_3 monitor, counts	589,463	1,137,485
Start of count, time after irradiation	2.00 min.	2.20 min
Counting time, live	10.00 min.	10.00 min.
" " , clock	10.08 min.	10.08 min.
Net counts, 3.1 Mev peak	1680	1421
" " , 1.15 " "	7293	577
Decay factors from end of irradiation to midpoint of count:		
8.8 min. Ca^{49} (3.1 Mev)	0.580	0.565
22 min. K^{44} (1.15 Mev)	0.800	0.795
Counting efficiencies, photopeak		
3.1 Mev	0.01	0.01
1.15 Mev	0.02	0.02
Disintegration rates, corrected to end of irradiation and normalized to 10^6 BF_3 monitor counts, dpm/gram of calcium,		
3.1 Mev	1.18×10^4	3.9×10^3
1.15 Mev	1.80×10^4	5.6×10^2
Saturation factors, 10 min. irrad.		
8.8 min Ca^{49}	0.544	0.544
22 min. K^{44}	0.271	0.271
Flux, [a] n/cm^2-sec:		
Thermal, from $Ca^{48}(n,\gamma)Ca^{49}$	1.17×10^7	3.90×10^6
Fast, from $Ca^{44}(n,p)K^{44}$	1.5×10^8	4.7×10^6

a) Calculated from: $A = N\sigma\phi S$,

where
- A = disintegrations per second per gram of calcium and is obtained by dividing dpm/g by 60,
- $N = 2.88 \times 10^{19}$ atoms Ca^{48}/g calcium, and $= 3.10 \times 10^{20}$ atoms Ca^{44}/g Ca,
- $\sigma = 1.1 \times 10^{-24} cm^2$ per atom Ca^{48} for (n,γ) reaction,
  $= 2.5 \times 10^{-26}$ cm^2 per atom Ca^{44} for (n, p) reaction with 14 Mev neutrons,
- S = saturation factor.

TABLE 21

Calculated Relative Standard Deviation of Calcium Determinations, Counting Statistics Only

Bone Weight, g	Calcium, g[a]	Calculated Standard Deviation[b]	
		% of Value	Calcium, g
1	0.2	± 17	± 0.034
3	0.6	± 9.6	± 0.058
10	2	± 5.3	± 0.106
30	6	± 3.0	± 0.180
100	20	± 1.7	± 0.340
300	60	± 0.1	± 0.660
1000	200	± 0.5	± 1.000
1500	300	± 0.4	± 1.200
2000	400	± 0.33	± 1.300

a) Assuming bone is 20% by weight calcium.

b) Including standard deviation contribution of comparator standard.

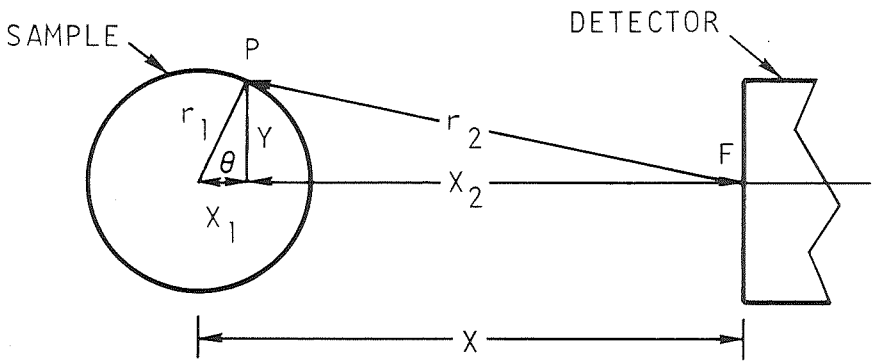

Figure 1. Counting geometry, ring sample

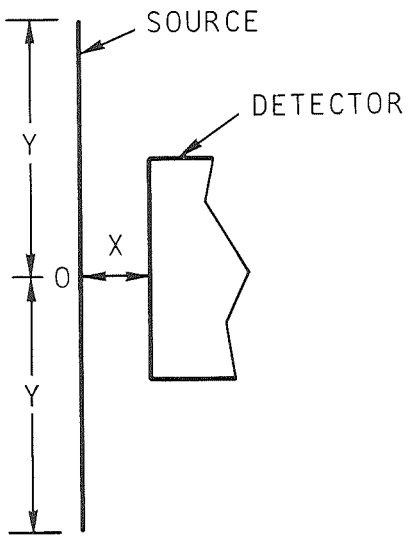

Figure 2. Counting geometry, line sample

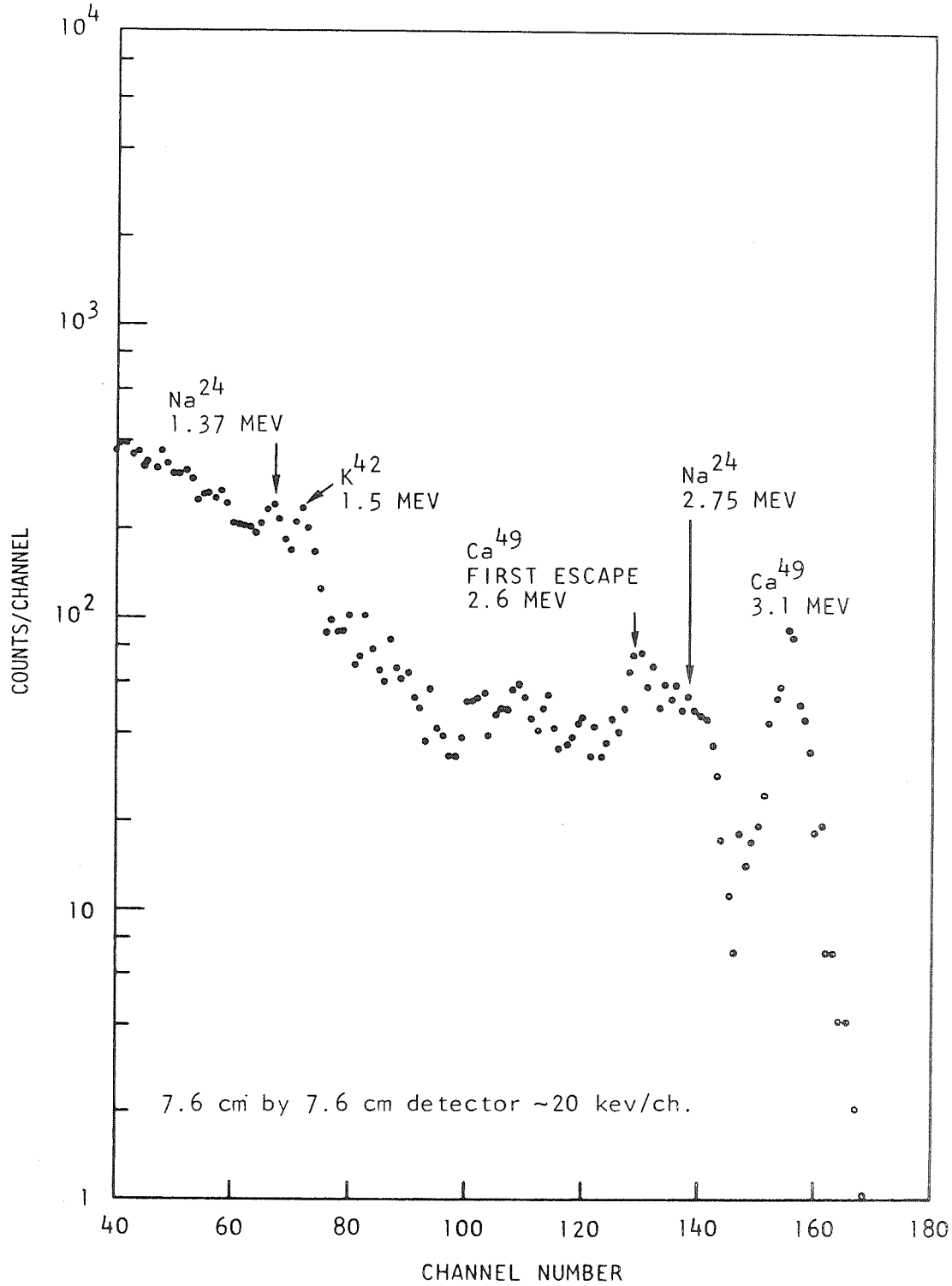

Figure 3. Gamma-ray spectrum of neutron-activated femur obtained in first series of experiments

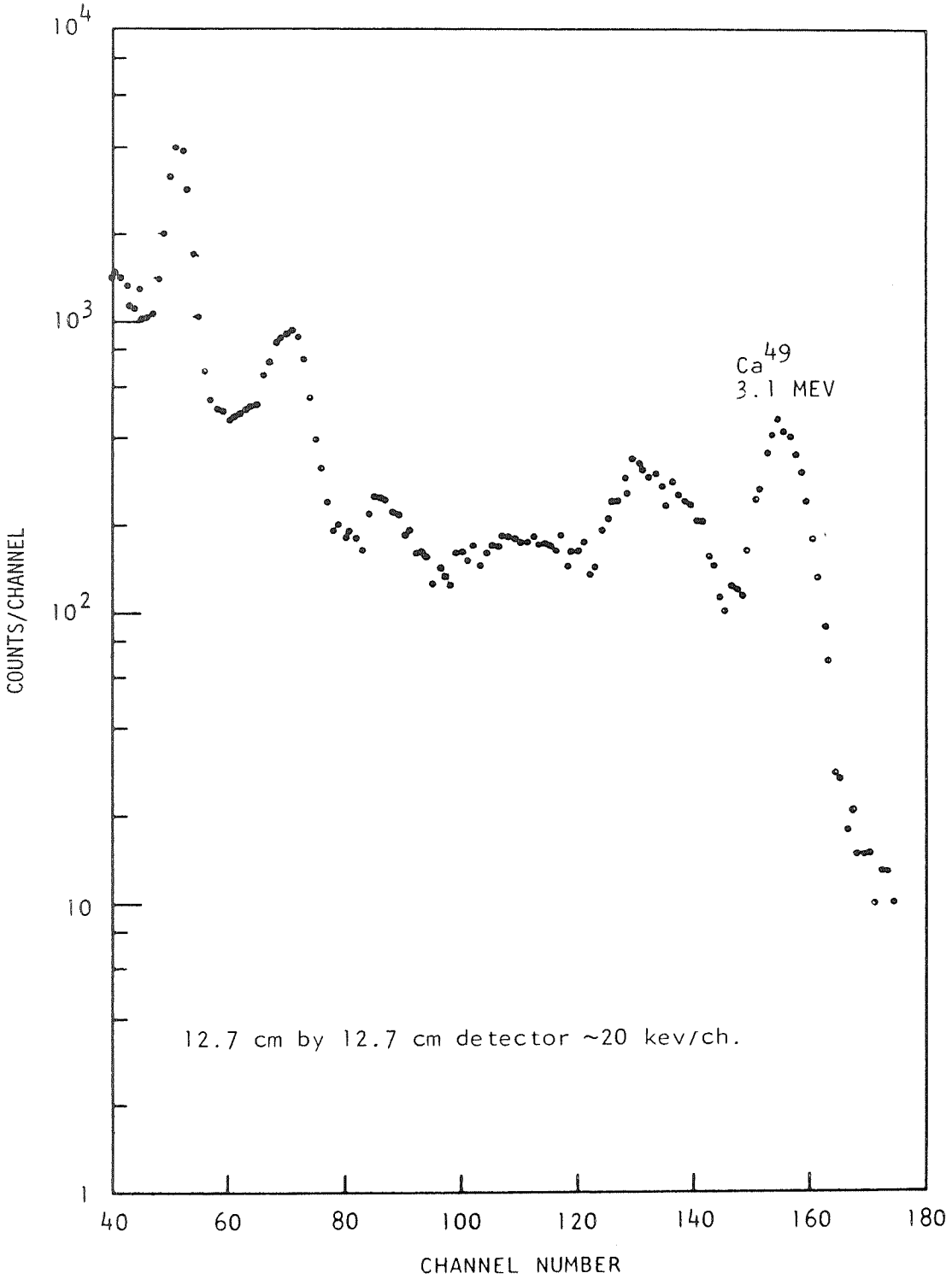

Figure 4. Gamma-ray spectrum of neutron-activated vertebra obtained in third series of experiments

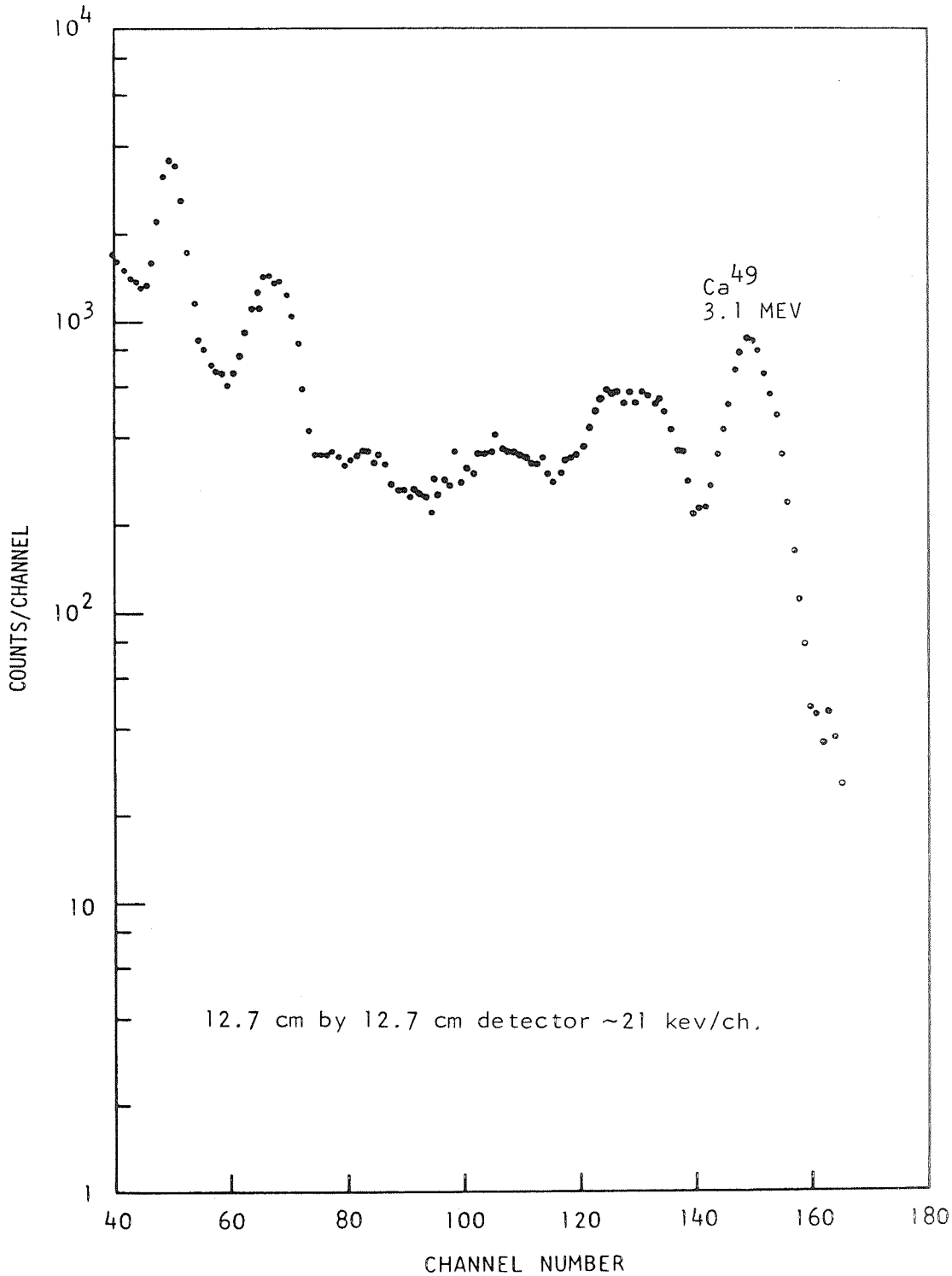

Figure 5. Gamma-ray spectrum of neutron-activated femur obtained in fourth series of experiments

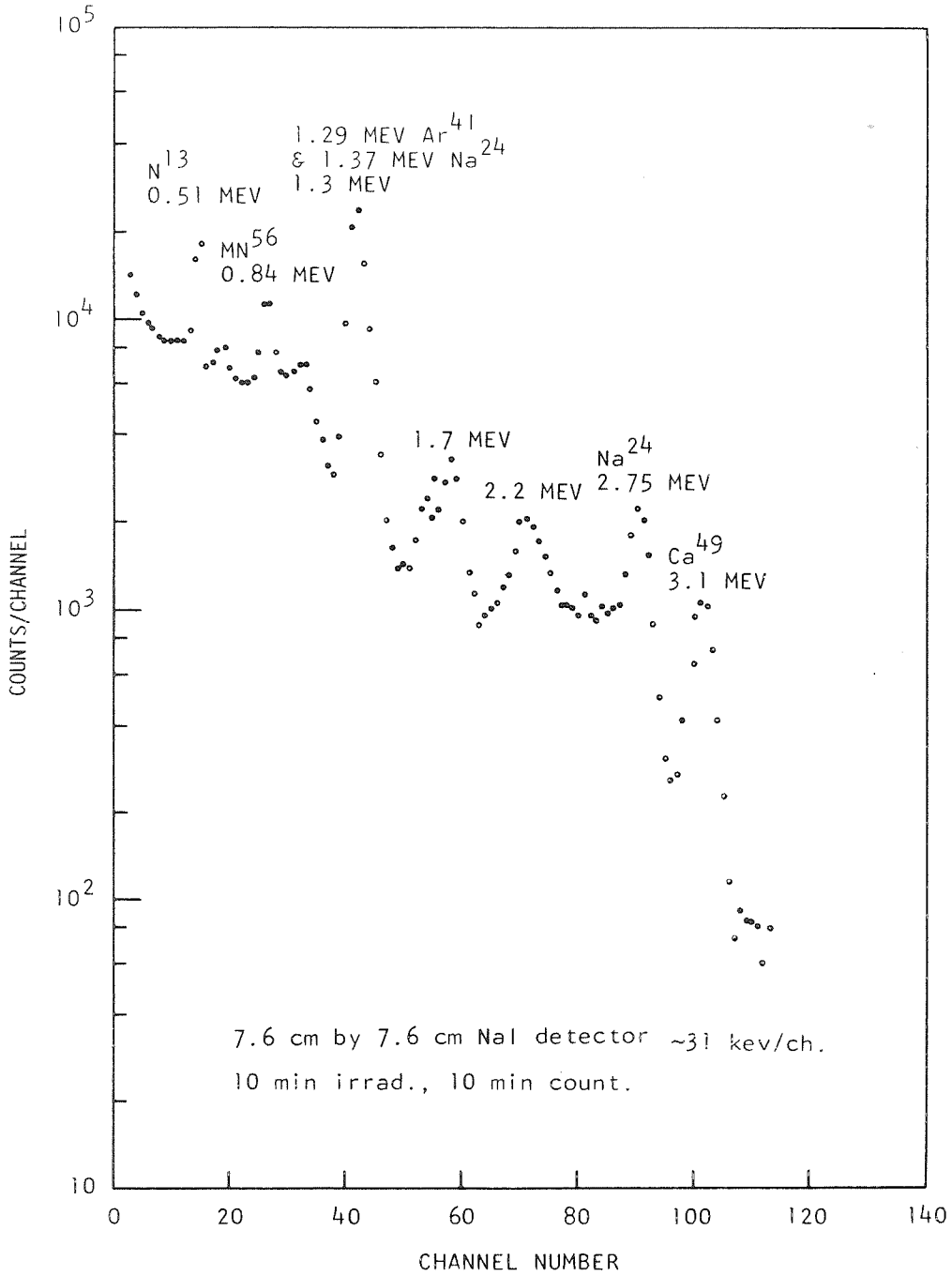

Figure 6. Gamma-ray spectrum of neutron-activated solution containing 5 μg of sodium and 50 μg of calcium

NASA-Langley, 1970 —— 5

"The aeronautical and space activities of the United States shall be conducted so as to contribute . . . to the expansion of human knowledge of phenomena in the atmosphere and space. The Administration shall provide for the widest practicable and appropriate dissemination of information concerning its activities and the results thereof."

—NATIONAL AERONAUTICS AND SPACE ACT OF 1958

NASA SCIENTIFIC AND TECHNICAL PUBLICATIONS

TECHNICAL REPORTS: Scientific and technical information considered important, complete, and a lasting contribution to existing knowledge.

TECHNICAL NOTES: Information less broad in scope but nevertheless of importance as a contribution to existing knowledge.

TECHNICAL MEMORANDUMS: Information receiving limited distribution because of preliminary data, security classification, or other reasons.

CONTRACTOR REPORTS: Scientific and technical information generated under a NASA contract or grant and considered an important contribution to existing knowledge.

TECHNICAL TRANSLATIONS: Information published in a foreign language considered to merit NASA distribution in English.

SPECIAL PUBLICATIONS: Information derived from or of value to NASA activities. Publications include conference proceedings, monographs, data compilations, handbooks, sourcebooks, and special bibliographies.

TECHNOLOGY UTILIZATION PUBLICATIONS: Information on technology used by NASA that may be of particular interest in commercial and other non-aerospace applications. Publications include Tech Briefs, Technology Utilization Reports and Notes, and Technology Surveys.

Details on the availability of these publications may be obtained from:

SCIENTIFIC AND TECHNICAL INFORMATION DIVISION

NATIONAL AERONAUTICS AND SPACE ADMINISTRATION

Washington, D.C. 20546